

SSS023-01

Room:IC

Time:May 23 08:30-08:45

## The nuclear power plant disaster accompanying a great earthquake and the plan to avoid the disaster

Kozo Takahashi<sup>1\*</sup>

<sup>1</sup>None

Nuclear disaster: Luckily or unluckily, we have already experienced nuclear accidents which suggest enough the nuclear disaster.

On March 28, 1979, at nuclear reactor No.2 of Three Mile Island, the core meltdown started six minutes after the fault of the main pump, because the outlet of the backup pump was closed. The evacuation in wide area carried out, because it was feared that both pressure vessel and reactor vessel would explode, and that radioactive dust would fall there, though the radiation was limited as the emergency core cooling system (ECCS) was intermittently operated.

This accident shows that the nuclear disaster may happen, even if the reactor is not operating.

On April 26, 1986, at the reactor No.4 of Chernobyl small nuclear explosion occurred when it started to insert all reactor control rods after the experimental operation at extremely low output power.

This disaster shows that the nuclear explosion may happen when a serious fault occurs or maloperation is carried, during the reactor is operating.

A standard 1Gw nuclear power plant (NPP) of Chubu Electric Power Co. at Hamaoka Japan, for example, when the acceleration of more than 0.15g is sensed, automatically inserts all control rods in 1.5 secs and stops the reaction before a S wave arrives.

Hamaoka plants can resist the shock of up to 2g. But we have experienced more than 2g. In S. Iwate Pref. Eq. (2008/06/13, M: 7.2, Depth: 8km), Tsubakidai St., which is located at the epicentral distance of 19km and at the hypocentral distance of 20.6km, observed the maximum acceleration of 4.1g. The distance between Hamaoka and the top surface of Philippine Sea Plate (PSP), where a great earthquake may occur, measures 15 - 20km. So, it is possible that Hamaoka plants experience more than 2g, and then main pipes are broken, and the loss of cooling water starts, though an ECCS is equipped to avoid the loss, because both probabilities of the break and the failure of ECCS are nearly the same. When cooling water leaks in large quantities, the core meltdown starts in a few minutes, even if the reaction has been stopped then, both pressure vessel and reactor vessel explode, like the reactor of Chernobyl did, and it might happen that the half of our population needs to evacuate, depending on wind direction.

In the case where main pipes are broken and the loss of cooling water starts, during the reactor is operating in full power, both pressure vessel and reactor vessel explode, which will be similar to a uranium bomb, and the magnitude of the disaster will be about 1000 times of that at Chernobyl. This is inferred from that at Chernobyl only one cell of 1661 cells exploded.

A plan to avoid the disaster: To avoid these disasters, it is necessary to predict great earthquakes. Before great earthquakes usually extraordinary electric fields have been observed. Before and after S. Suruga Bay Eq. (2009/08/11, M: 6.5, Depth: 23km), anomalous electric pulses were also found. In the case the prediction system that monitor the precursory pulses is established, which can use a lightning location system in common, when a great earthquake of more than magnitude 8 occurs, not only the disaster is prevented by stopping NPP following to the precursor, but also NPP can continue to operate without stopping the plant wastefully for long time when it is clear that the distance to the predicted source region is 100km or more, which is measured as the pulses are located at the accuracy of 10km, and that the magnitude, which is estimated from the quantity of the pulses, is less than 8.

Keywords: nuclear power plant disaster, great earthquake, earthquake directly under the plant

# Japan Geoscience Union Meeting 2011

(May 22-27 2011 at Makuhari, Chiba, Japan)

©2011. Japan Geoscience Union. All Rights Reserved.



SSS023-02

Room:IC

Time:May 23 08:45-09:00

## Transdisciplinary Study on Earthquake-related Diseases (7) For Improving Emergency Ambulance Activities

Yutaka Ohta<sup>1\*</sup>

<sup>1</sup>Tono Research Inst of Earthq Science

Under a major title as above we have recently been studying for optimization of ambulance activities at an attack by a significant earthquake. This is just continuous study report. Mizunami city, Gifu prefecture, as a sample area in this study, where our Institute locates, has been operating 3 ambulances and it is in higher level than that of the Japan standards. The activities in ordinary situation are therefore satisfactory as to be able to cover 80 or higher percentage of responses to emergency phone calls by 119. In case when a large earthquake attacks, however, the ambulance activities available get down as low as 10% in immediate stages, and therefore any improvement as either reduction of calls by 119 or quicker turn-around time service of ambulance activity is expected. From this point, we introduced probable strategies via simulation in a previous study. But, no detail examination was introduced to know whether the proposed strategies work well or not. This paper pays special effort for examining the reality of the proposed strategies, obtaining additional field data from the sample area.

What found via the analyses of ambulance activity data are that the ambulance dispatches for lightly suffered patients is still over weighted, and we should recall the primary role of ambulance activities. It is nothing but an activity to assist life saving in emergency situations. In this respect we arrive at a conclusion that no lightly suffered citizens are to be transported in use of a limited number of ambulances, especially in unusual situation as an earthquake attack.

Keywords: Earthquake-related Health Consequences, Seriousness Level, Ambulance Activity, Call-response Rate, Simulation

SSS023-03

Room:IC

Time:May 23 09:00-09:15

## Benchmark Tests for Strong Ground Motion Simulations (Part 6: Theoretical Methods, Step 3 & 4)

Yoshiaki Hisada<sup>1\*</sup>, Masayuki NAGANO<sup>2</sup>, Atsushi, NOZU<sup>3</sup>, Ken MIYAKOSHI<sup>4</sup>, Taro NAKAGAWA<sup>5</sup>, Kimiyuki ASANO<sup>6</sup>

<sup>1</sup>Kogakuin University, <sup>2</sup>Tokyo University of Science, <sup>3</sup>The Port and Airport Research Institute, <sup>4</sup>Geo-Research Institute, <sup>5</sup>Fujita Corporation, <sup>6</sup>Disaster Prevention Research Institute

We have been conducting a series of benchmark tests of the strong motion simulation methods for three years since 2009. We chose the three most popular methods for this purpose: the theoretical methods (the wavenumber integration method, the discrete wavenumber method, and the thin-element method), the stochastic Green function method, and the numerical methods (the finite difference method and the finite element method). In this presentation, we show the results of the theoretical methods for the steps 3 and 4; the former is a point source and the latter is extended sources in flat-layered structures, as shown in the tables 1 and 2.

We have obtained the following conclusions. All the results show good agreements in the assigned frequency range (0 - 5 Hz). However, the results for no-damping media show slight differences at very high frequencies, because some groups used very high-Q values, whereas the other group used the Phinney method. In addition, there are slight differences for the a point source on the free surface and the surface faulting model. This is because that the some use the exact surface source model, and the other used the source slightly under the surface.

Please check the following web site for more details.

<http://kouzou.cc.kogakuin.ac.jp/benchmark/index.htm>

### Acknowledgements:

This project is in part supported by a research fund of Ministry of Education, Culture, Sports, Science and Technology of Japan (MEXT), and the Research Center of Urban Disaster Mitigation (UDM) of Kogakuin University.

Table 1 Benchmark tests for the 2010 theoretical methods (Step 3 and 4)

ステップ3 (締切:2010/9/1)			ステップ4 (締切:2010/11/1)				
モデル名	T31	T32	T33	T41	T42	T43	T44
地盤	4層地盤		2層地盤	2層地盤			
減衰	あり		なし	あり			
震源	点震源 (深さ 2 km : ガウス型開数)		点震源 (深さ 0 km : ガウス型開数)	横ずれ断層 (上端深さ 2 km : 中村-宮武開数)		横ずれ断層 (上端深さ 0 km : 中村-宮武開数)	
有効振動数	0~5 Hz						
出力点	+002, +006, +010, +030, +050, +100 km (計 6 点)						
				破壊伝播	1km <sup>2</sup> 間隔一定	1km <sup>2</sup> 間隔ゆらぎ	連続
	0~5 Hz						
	出力点 ±002, ±006, ±010, ±030, ±050, ±100 km (計 12 点)						
				推出波形	1波形	3波形	1波形

Table 2 Material Properties for the four layered model

Layer	Thickness (m)	Vp(m/s)	Vs(m/s)	Density(kg/m <sup>3</sup> )	Qp	Qs
1	200	1,800	400	2,000	20f	20f
2	400	2,600	1,000	2,400	30f	30f
3	1,000	4,000	2,000	2,600	40f	40f
4 (Half Space)	∞	6,000	3,464	2,700	70f	70f

注1: Q 値の f は振動数(Hz) 注2: 2層地盤モデルの場合、第3層を厚さ 1 km とする

Keywords: Strong Ground Motion Simulations, Benchmark Test, Theoretical Methods, Wavenumber Integration Method, Discrete Wavenumber Method, Thin Layer Method

SSS023-04

Room:IC

Time:May 23 09:15-09:30

## Benchmark Tests for Strong Ground Motion Simulations (Part 7 : Numerical Methods, Step 3 & 4)

Chiaki Yoshimura<sup>1\*</sup>, M. Nagano<sup>2</sup>, S. Aoi<sup>3</sup>, H. Kawabe<sup>4</sup>, H. Uebayashi<sup>4</sup>, T. Hayakawa<sup>5</sup>, S. O. Citak<sup>6</sup>, Y. Hisada<sup>7</sup>

<sup>1</sup>Taisei Co., <sup>2</sup>Tokyo Univ. of Science, <sup>3</sup>NIED, <sup>4</sup>Kyoto University, <sup>5</sup>Shimizu Co., <sup>6</sup>JAMSTEC, <sup>7</sup>Kogakuin Univ.

We performed a benchmark test for the strong motion simulation methods using numerical methods (finite differences method and finite element method). Six teams from different institutions solved the same problems with the same subsurface structure models and the same seismic sources. We tested three subsurface models: a four layers model, a torapezoidal sedimentary basin model and a stant basement model. All the results calculated by six teams generally show good agreement to each other. We found minor differences are generated by the difference of property distribution near the irregular layer boundaries.

表 1 2010 年度の数値解析手法の解析条件一覧

モデル名	ステップ3 (締切:2010/9/1)			ステップ4 (締切:2010/11/1)	
	N31	N32	N33	N41	N42
地盤	4層地盤		対称盆地	傾斜基盤盆地	
減衰	あり			あり	
震源	点震源A	点震源B	点震源C	点震源C	点震源D
有効動数	0~2.5Hz			0~2.5Hz	
出力点	21点	19点	21点	21点	21点

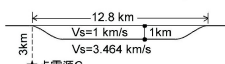
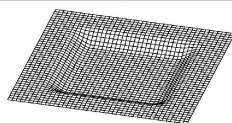


図1 対称盆地 (N33)

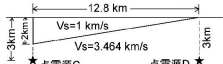
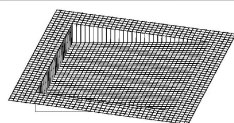


図2 傾斜基盤盆地 (N41, N42)

Keywords: Strong Ground Motion Simulation, Benchmark Test, Numerical Methods, Finite Difference Method, Finite Element Method

SSS023-05

Room:IC

Time:May 23 09:30-09:45

## Benchmark Tests for Strong Ground Motion Simulations (Part 8: Stochastic Green's Function Method, Step 3 & 4)

Kenichi Kato<sup>1\*</sup>, Yoshiaki Hisada<sup>2</sup>, Susumu Ohno<sup>3</sup>, Arihide Nobata<sup>4</sup>, Atsushi Morikawa<sup>1</sup>, Yu Yamamoto<sup>5</sup>

<sup>1</sup>Kobori Research Complex, <sup>2</sup>Kogakuin Univ., <sup>3</sup>Tohoku Univ., <sup>4</sup>Obayashi Co., <sup>5</sup>Taisei Co.

Since 2009, we performed a benchmark test for the strong motion simulation methods as three years project (Hisada et al., 2011; Yoshimura et al., 2011; Kato et al., 2011). This paper shows the results using stochastic Green's function method.

We have carried out two steps of simple benchmark tests in 2009; one is a point source (step 1) and the other is extended sources (step 2) in homogeneous and two-layered subsurface structures. Radiation coefficient of the source is assumed to be frequency independent, and only SH wave is considered. Site amplification is calculated assuming normal incidence of SH wave. Six groups of researchers/engineers were participated in by using their own methods/codes. Since the simple model is used in the step 1 and 2, all the results calculated by six teams generally show good agreement to each other (Kato et al., 2011).

In step 3 and step 4, more complicated analytical conditions are considered as shown in Table 1. Frequency dependent radiation coefficient of the source is applied, which is the most different conditions in comparisons with step 1 and step 2. Since oblique incidences of both SH and SV waves are considered, vertical component is also generated in addition with horizontal components. All the results of the point source (step 3) and the extended sources (step 4) generally show good agreement to each other in spite of complicated analytical conditions. As for the step 4, we confirmed that the introduction of the random rupture times at the sub-faults are effective to avoid the artificial predominant frequencies caused by the regular intervals of the rupture times. We also found the serious sags in Fourier amplitudes in the middle frequency range around 1 Hz, as compared with the omega-squared model. Since the sags underestimate synthesized amplitude, this problem has to be improved in the future. Synthesized amplitude shows variation in particular frequencies, because random numbers are used in generating time histories and so on. When applying the stochastic Green's function method, this variation should be in mind. Please check the following web site for more details.

<http://kouzou.cc.kogakuin.ac.jp/test/home.htm>

### Acknowledgments:

This project is in part supported by a research fund of Ministry of Education, Culture, Sports, Science and Technology of Japan (MIEXT), the Research Subcommittees on the Earthquake Ground Motion of the Architectural Institute of Japan, and the Research Center of Urban Disaster Mitigation (UDM) of Kogakuin University.

### References:

Hisada et al., benchmark tests for strong ground motion prediction methods -Case for theoretical methods (Part 1)-, AIJ J. Technol. Des. Vol. 17, No.35, 43-48, 2011.

Kato et al., benchmark tests for strong ground motion prediction methods: Case for stochastic green's function method (Part 1), AIJ J. Technol. Des. Vol. 17, No.35, 49-54, 2011.

Yoshimura et al., benchmark tests for strong ground motion prediction methods: Case for numerical methods (Part 1), AIJ J. Technol. Des. Vol. 17, No.35, 67-72, 2011.

Table 1 Benchmark tests for stochastic green's function method in 2010

モデル名	ステップ3 (点震源)				ステップ4 (面震源)			
	S31	S32	S33	S34	S41	S42	S43	S44*
地盤	一様地盤	2層地盤		4層地盤	2層地盤			
入射角	鉛直	斜め入射			斜め入射			
Q値	なし	あり			あり			
震源	点震源				横ずれ断層	逆断層	横ずれ断層	
干渉イオン (SH & SV)	振動数 (f) 一定		振動数 (f) 依存		振動数 (f) 依存			任意
破壊開始時間					一定	ランダム	一定	
有効振動数	0~20 Hz				0~20 Hz			
出力点	000, +002, +006, +010 (計4点)				000, ±002, ±006, ±010 (計7点)			
出力成分	水平2成分	水平・上下3成分			水平・上下3成分			
乱数の設定	各自の乱数3パターン				各自の乱数3パターン			

注\*) S44はオプションケースで自由参加。近地項や中間項の考慮など各自のオリジナル手法を考慮

Keywords: Strong motion prediction methods, Benchmark tests, Stochastic Green's function method, Random numbers, Point source, Fault model

SSS023-06

Room:IC

Time:May 23 09:45-10:00

## Ground motion duration and earthquake magnitude

Tetsu Masuda<sup>1\*</sup>

<sup>1</sup>ERI, University of Tokyo

Stochastic Green's function method is one of the useful tools to calculate ground motions. To account for the effects of asperities and rupture propagation, the entire fault of dimension  $L$  is sub-divided into small sub-faults of dimension  $R$ , and ground motions from all sub-faults are integrated instead of evaluating from a point source. Though the size of element is arbitrary, the final synthesized ground motion must not depend on the sub-fault size. Stochastic Green's function is based on the product of Gaussian time series and envelope shape function  $e(t)$ . In many cases, duration  $T_r$  of the envelope shape function is set as inversely proportional to the corner frequency  $f_c$  of sub-fault, or in other words, as proportional to the dimension of sub-fault  $R$ .

$$T_r = d/f_c = (d/C_c)(R/V_s) \dots (1)$$

When a point source is assumed, total duration of ground motion  $T$  is coincide with the envelope function duration,

$$T = T_r = (d/C_c)(L/V_s) \dots (2)$$

The total duration of synthesized ground motion  $T$  is the sum of time for the rupture  $T_p$  to propagate the entire fault and the duration of sub-fault ground motion  $T_r$ .

$$T_p = C_p(L/V_s) \dots (3)$$

$$T = T_p + T_r \dots (4)$$

Generally, equation (2) for a point source and equation (4) for finite source give different values of ground motion duration. As the sub-fault size gets small, the sum also gets small, and the synthesized ground motion does depend on the sub-fault size. Ground motion duration is dependent not only on terms related to the seismic source, such as rupture propagation time  $T_p$  and sub-fault duration  $T_r$ , but also on terms  $T_m$  attributed to the medium, such as reflections and scattering. Therefore, the ground motion duration is expressed as,

$$T = T_m + T_p + T_r \dots (5)$$

As the entire fault size  $L$  increases as the earthquake magnitude increases, the total duration of ground motion also increases as the magnitude increases. Equation (5) gives a different relationship between ground motion duration and magnitude from equation (2).

In order to clarify which is more acceptable, I investigated the dependency of ground motion duration on earthquake magnitude. I analyzed big earthquakes and their aftershocks which recently occurred in and around Japan. They include shallow crustal earthquakes, inter-plate earthquakes, and intra-plate earthquakes. The magnitude ranges from 3.6 to 8.0. The observed records from K-NET and KiK-net of NIED and JMA are used. There is variety of definition of ground motion duration. In this paper, I adopted the  $T_w$  defined in Boore's envelope shape function, accounting for stochastic Green's function method for strong ground motion prediction.

$$e(t) = a t^b \exp(-ct), t > T_s \dots (6)$$

$$T_w = b/c/0.2 \dots (7)$$

where  $t$  is time, the parameters  $a$ ,  $b$ , and  $c$  determines the envelope shape,  $T_s$  is the arrival time of S wave. Equation (6) is fit to the envelope of observed records of each observation and from each earthquake, the unknown parameters  $a$ ,  $b$ ,  $c$ , and  $T_s$  being determined by the least squares method. The duration of ground motion is calculated by using equation (7).

The following results are obtained.

1. Ground motion duration strongly depends on epicentral distance.
2. Ground motion duration depends on earthquake magnitude.
3. Ground motion duration also depends on velocity structure near the observation station. Longer duration is observed for longer characteristic period of ground.
4. For earthquakes with small magnitude, ground motion duration is not so short as expected from equation (4).
5. Equation (5) better explains the observed ground motion duration.

Keywords: ground motion duration, earthquake magnitude, rupture propagation, rise time, strong ground motion prediction, stochastic Green's function

SSS023-07

Room:IC

Time:May 23 10:00-10:15

## Multi-GPU-accelerated simulation of seismic wave propagation for models with land-ocean topography

Taro Okamoto<sup>1\*</sup>, Hiroshi Takenaka<sup>2</sup>, Takeshi Nakamura<sup>3</sup>, Takayuki Aoki<sup>1</sup>

<sup>1</sup>Tokyo Institute of Technology, <sup>2</sup>Kyushu University, <sup>3</sup>JAMSTEC

Accurate simulations of seismic wave propagation using the heterogeneous Earth model is essential in evaluating the strong ground motions due to earthquakes. Recent study with realistic models of land topography and oceanic layer have been revealing their effects on the seismic ground motions (e.g., Nakamura et al., AGU Fall Meeting, 2009). Thus the effects of the land-ocean topography need be incorporated in the simulations and be studied further for better understanding of the ground motions. In order to include those effects, we have recently proposed a unified approach (Takenaka, SEGJ 2009) to model structures with both the irregular free-surface (i.e., land topography) and the irregular water-solid interface (e.g., ocean bottom) in 3D seismic modeling with the finite-difference method (FDM). The approach allows to incorporate the effect of land-ocean topography with sufficient accuracy.

Thus, we implement the unified approach into multi-GPU finite-difference method (FDM) program. The GPUs are adopted to accelerate the simulations because, not only the accuracy, but also the efficiency (performance) of the numerical method is important for the simulation of the seismic wave propagation. GPU (Graphics Processing Unit) is a remarkable device for its many core architecture and for its high memory bandwidth. Recent GPU delivers extremely high computing performance (more than one TFlops in single-precision arithmetic) at a reduced power and cost compared to conventional CPUs.

In this talk we present examples of the simulations by using the new TSUBAME-2.0 grid cluster in the Global Scientific Information and Computing Center, Tokyo Institute of Technology. TSUBAME-2.0 is equipped with 4,224 NVIDIA M2050 GPUs and is ranked as world fourth fastest supercomputer in the recent TOP-500 list. Our MPI-parallel FDM program with the three-dimensional domain decomposition have achieved a performance of about 42.7 TFlops by using 1,200 GPUs so far. The weak scaling was nearly proportional to the number of the GPUs. We will also present some examples of visualization of the wave propagation for realistic land-ocean model.

Keywords: GPU, seismic wave propagation, finite-difference method, topography, ocean bottom topography



SSS023-08

Room:IC

Time:May 23 10:15-10:30

## Low-frequency seismic wave simulation with tuned 1-D structure

Tatsuhiko Saito<sup>1\*</sup>, Youichi Asano<sup>1</sup>, Yoshihiro Ito<sup>2</sup>, Katsuhiko Shiomi<sup>1</sup>

<sup>1</sup>NIED, <sup>2</sup>Tohoku University

High-quality seismograms recorded by nation-wide seismic network, Hi-net, provide a good opportunity for examining our understanding of earthquake related phenomena, or the performance of the quantitative modeling. The purpose of this study is to examine the performance of 1-D velocity structure models for simulating low-frequency (0.02 - 0.05 Hz) seismic wavefield. We investigated the performance of the conventional 1-D velocity structure model which is used for the estimation of CMT solution in Japan, and a new 1-D velocity model we proposed in this study.

First, we proposed a new 1-D velocity model based on the dispersion relations for Rayleigh and Love waves. The dispersion relations were obtained by the array analysis of Hi-net records of huge teleseismic events ( $M > 8.0$ ). Although the conventional model fails to reproduce the observed dispersion relations, a new model which is characterized by 4 % decrease in S-wave velocities in crust and 2 % decrease in mantle can reproduce the observed dispersion relation well in the frequency range of 0.01 Hz - 0.1 Hz for both Rayleigh and Love waves.

Then, we confirmed the superiority of the new model in the point of the performance of simulating low-frequency (0.02 - 0.05 Hz) seismic-wave propagation over Japan from large earthquakes ( $6.0 < M < 6.8$ ). We confirmed that the new velocity model was able to simulate the observed seismograms better than the conventional velocity model for many earthquakes. The new model, in particular, can simulate better the travel times of surface waves for long epicentral distance ( $> \sim 400$  km). Furthermore, the centroid times obtained by the new model are systematically ( $\sim 2$  sec) earlier than those by the conventional model.

Through this study, we proposed a new 1-D velocity model, which have better performance for simulating low-frequency seismic waves than the conventional model. The performance of the simulation is significantly improved for many cases but not for all the earthquakes we analyzed. For example, when the surface waves passing through Hida Mountains, the central part of Japan, we cannot well simulate the seismograms. To overcome this limitation, it would be important to extend the velocity model to have spatial varying Moho.

Keywords: Seismic wave, Simulation

SSS023-09

Room:IC

Time:May 23 10:45-11:00

## Spectral Amplification Factors for Long-Period (3 to 10 s) Ground Motions in and around the Los Angeles Basin during the

Ken Hatayama<sup>1\*</sup>, Erol Kalkan<sup>2</sup>

<sup>1</sup>Nat'l Res. Inst. of Fire and Disaster, <sup>2</sup>U.S. Geological Survey

Mw7.2 El Mayor-Cucapah earthquake that occurred near the U.S.-Mexico border on April 4, 2010 is the first event providing a number of high-quality recordings to study long-period (3 to 10 s) ground motion amplification in and around the Los Angeles (LA) basin. In the LA basin, about 300 km away from the source, higher PGV values ( $\sim 0.1$  m/s) of long-period ground motions were observed relative to its surrounding area. By using more than 200 records from this event, spectral amplification factors of long-period ground motions were evaluated in and around the LA basin with respect to reference hard-rock sites. The main observations of this evaluation are the following: (1) Relative to the hard-rock reference sites, the maximum amplification is about a factor of 5 at 8 and 10 s periods in the central part of the LA basin, where depths of  $V_s$  3.2 km/s and  $V_s$  2.8 km/s isosurface according to the latest Southern California Earthquake Center Community Velocity Model (SCEC CVM-H 6.2) are correlated strongly with the observed high amplification; (2) in the San Gabriel valley, located northeast of the LA basin, the maximum amplification is about a factor of 3 at 8 s, and it is correlated well with the depth of  $V_s$  1.5 km/s isosurface; (3) the largest amplification reached to a factor of 10 at the 6 s in the western part of the LA basin (Manhattan Beach), where the SCEC CVM-H 6.2 failed to provide the feature of the underground structures corresponding to the observed high amplification. The observations (1) and (2) mean that there is no single  $V_s$  isosurface that represents spatial variations of the long-period ground motion amplification observed in and around the LA basin. Finally, we compared the spectral amplification factors from the observations with those from the simulations using a simple point-source model and the SCEC CVM-H 6.2. Although the simulation results generally agree with the observations for spatial variation of amplification factors at long periods over 8 s, they tend to overestimate the intensity of amplification factors. Including Q-values and/or using detailed source model might improve the agreement between simulations and observations.

Keywords: long-period ground motions, Los Angeles basin, El Mayor-Cucapah earthquake, spectral amplification factors

SSS023-10

Room:IC

Time:May 23 11:00-11:15

## 3-D underground structure model and simulation of seismic motions in the Mikawa area, Aichi prefecture

Koichiro Saguchi<sup>1\*</sup>, Kazuaki Masaki<sup>2</sup>

<sup>1</sup>Nihon Emsco Ltd., Co., <sup>2</sup>Aichi Institute of Technology

Mikawa area is one of the most eminent industry one in Japan and when Tokai and Tonankai earthquake will occur in the near future, it concerned that large economic and human loss will happen in this area. However, three dimensional under ground structural model is not clear still enough for the estimation of the strong ground motions in this area. In this study, we constructed the seismic observation net (Ai-net) in the Mikawa area and we estimated the three dimensional under ground structural model using the receiver function method from the obtained records at Ai-net To accomplish it, we simulated seismic ground motions at observation sites at the Ai-net using the three-dimensional finite element method

The seismic ground motion array observation has been continued after 2005 in the Miakwa area. Acceleration type strong motion seismometers with three components were installed at 30 sites in this area. We calculated the receiver functions from 7 seismic records obtained at each station, and we identified the underground structural model using the simulated annealing method (Ingber (1989)). Based on numerical experiments it is indicated that P-wave velocities, S-wave velocities and Q values of individual layers are inverted very well. Moreover, we constructed the three dimensional under ground structural model in this area obtained from P-wave and S-wave velocity profiles of thick sediments at each station.

Finally, we simulated seismic ground motions at observation sites at the Ai-net using the three-dimensional finite element method considering three-dimensional velocity structure down to 10km. The results indicate that the maximum accelerations in simulated waveforms were similar to the observed one.

Keywords: 3-D underground structural model, simulation of the seismic ground motion, finite element method, seismic observation

SSS023-11

Room:IC

Time:May 23 11:15-11:30

## Estimation of Rayleigh wave group velocity in the 1891 Nobi earthquake fault system using seismic interferometry

Hiroaki Sato<sup>1\*</sup>, Masayuki Kuriyama<sup>1</sup>, Yasuhira Aoyagi<sup>1</sup>, Yoshiaki Shiba<sup>1</sup>, Sadanori Higashi<sup>1</sup>

<sup>1</sup>CRIEPI

During the 1891 Nobi earthquake, it was well known that the successive rupture of some major active faults have occurred about 80 km long in the NE-SW direction. In order to investigate a triggering mechanism of successive rupture of several active faults, it is important to estimate seismic velocity structure in the fault area of this earthquake. In the previous study we have used seismic tomography to estimate velocity structure in the northern part of the 1891 Nobi earthquake fault area by the microearthquake observation. In this research we tried to estimate Rayleigh wave group velocity in the above area using seismic interferometry by a long-term continuous measurement of microtremors.

The three-month continuous measurements of microtremors are conducted at 19 sites in and around the 1891 Nobi earthquake fault system with a receiver spacing of from about 10 to 20 km. The data were processed with seismic interferometric procedure to retrieve Green's function between receivers. We are successful to extract Green's function from stacking of cross-correlation between the two measurements sites using over 30 days of data. The dispersive characteristics of Rayleigh wave were found in the vertical component of observed Green's function of the period range from 0.5 to 8 sec using multiple filter technique. The group velocities of Rayleigh wave in the northern part of the 1891 Nobi earthquake fault area were estimated from the group delay time of two station pairs. As a result, the group velocity between the receivers in the northwestern part of this area (along the Nukumi fault) is high in the period range from 1 to 3 sec and the same in the period range over 3 sec compared to the one in the southwestern part (along the Neodani and Ibigawa fault). In the station pairs across the step between the Nukumi and Neodani fault, the low group velocity is derived in the period range from 3 to 6 sec. These results are able to be well explained by the previous results from seismic tomography.

Keywords: the 1891 Nobi earthquake, Seismic interferometry, Microtremor, Group velocity, Active fault

SSS023-12

Room:IC

Time:May 23 11:30-11:45

## H/V spectral ratio of microtremors and velocity structure in the Mexico basin

Shinichi Matsushima<sup>1\*</sup>, Takanori Hirokawa<sup>2</sup>, Yuhei Nitta<sup>2</sup>, Fumiaki Nagashima<sup>2</sup>, Francisco J. Sanchez-Sesma<sup>3</sup>, Hiroshi Kawase<sup>1</sup>

<sup>1</sup>DPRI, Kyoto University, <sup>2</sup>Grad. School Eng., Kyoto University, <sup>3</sup>Instituto de Ingenieria, UNAM

It is essential to detect the subsurface velocity structure beneath urban area to mitigate seismic disaster. In order to estimate the velocity structure, we have proposed a new theory to calculate the H/V spectral ratio assuming that wave propagation is completely diffuse. We measured microtremors in five sites in the Mexico basin, where there were severe damage during the 1985 Michoacan Earthquake several hundreds of kilometers away from the source region, to obtain data so that we can compare the observed H/V spectral ratios to the theoretical ones to check if our theory is applicable. Among the three stations observed in downtown Mexico City which are in a 1km range from east to west, at the most western site Plaza Cibeles, the H/V spectral ratio of NS and EW components look alike and has a peak of about 0.6Hz. The middle site Plaza Rio de Janeiro has a peak of about 0.5Hz for both NS and EW components. Jardin Pushkin, the most eastern site has two peaks for NS component, 0.5 and 0.7Hz respectively, and for EW component the peak is at 0.6Hz. Previous studies show that the predominant frequency for H/V spectral ratio of strong motions at Plaza Ciberes is about 0.5Hz (Salinas, 2010). On the other hand, the peak at Coyoacan, which is in the south part of Mexico City, is around 1.4Hz for NS and EW components and at CENAPRED, which is sitting on lava outcrop has no apparent peak. We will make detail analysis of the data and compare with the theoretical H/V spectral ratio calculated by our new theory from previously known velocity structures.

Keywords: Mexico Basin, Microtremor, H/V Spectral Ratio, Diffuse Field, Velocity Structure

SSS023-13

Room:IC

Time:May 23 11:45-12:00

## Site amplification factors derived from coda normalization method (4) amplification factors at borehole and surface

Teito Takemoto<sup>1\*</sup>, Takashi Furumura<sup>2</sup>, Takuto Maeda<sup>2</sup>, Shinako Noguchi<sup>2</sup>

<sup>1</sup>ERI, the Univ. of Tokyo, <sup>2</sup>CIDIR, the Univ. of Tokyo

### Introduction

We have estimated broad band ( $f = 0.5$ -1, 1-2, 2-4 and 4-8 Hz) site amplification factor at each site of the KiK-net and F-net strong motion network in Japan based on the coda normalization method. Estimated amplifications are applied for shaking intensity to show the validity of our estimates on the site amplification factors at each site and in frequencies (Takemoto *et al.*, 2009). Comparison between free surface and borehole in Northeastern Japan revealed that site amplification factors dramatically differ over 2 Hz (Takemoto *et al.*, 2010).

In this study, we used simultaneous inversion of KiK-net borehole and surface stations and F-net stations in whole of Japan to discuss S-wave amplification characteristic at borehole and surface stations in quantitative form.

### Data and Method

We used KiK-net surface and borehole stations and F-net nation-wide strong motion network developed across Japanese Islands. Using waveform data of acceleration record from 48 moderate earthquakes, we estimated the site amplification characteristic at each station in four frequency bands ( $f = 0.5$ -1 Hz, 1-2 Hz, 2-4 Hz, and 4-8 Hz).

The distribution of the site amplification characteristic in each frequency bands has been estimated by inversion. We assumed an F-net broadband seismic observation station installed in the basement rock site as unity (0 dB) site amplification.

### Results

In the high-frequency band ( $f = 4$ -8 Hz), absolute value of the site amplification factor in the borehole is smaller than that of the on free surface. Site amplifications in borehole concentrate around 0 dB. The spatial distribution pattern of the site amplification factor is poor correlated between free surface and in the borehole (correlation coefficient  $r = 0.52$ ). High-frequency wave has short wavelength and affected by small scale ( $< 100$ -200 m) structure.

On the other hand, there is little difference between spatial distribution of site amplification factor at borehole and surface stations ( $r = 0.88$ ) in low frequency band ( $f = 0.5$ -1 Hz). A few stations showed very high amplification ( $> 20$  dB) in both surface and borehole. Some stations showed small amplification around 0 Hz. Site amplifications in low frequency band have large deviation.

### Acknowledgement

We acknowledge the National Research Institute for Earth Science and Disaster Prevention, Japan (NIED) for providing the KiK-net and F-net waveform.

Keywords: coda normalization, site amplification

SSS023-14

Room:IC

Time:May 23 12:00-12:15

## Spatial interpolation of empirical amplification factors for response spectra of long-period ground motions

Toshimi Satoh<sup>1\*</sup>, Izuru OKAWA<sup>1</sup>, Takao NISHIKAWA<sup>3</sup>, Toshiaki SATO<sup>4</sup>

<sup>1</sup>Ohsaki Research Institute, <sup>2</sup>Building Research Institute), <sup>3</sup>Tokyo Metropolitan University, <sup>4</sup>Shimizu Corporation

We (Satoh et al, 2010) developed attenuation relations of acceleration response spectra with a damping factor of 5 % in a period range from 0.1 to 10 seconds including long period using many strong motion records observed at about 1870 stations to make design spectra for long-period structures. In the attenuation relations, amplification factor at each station was obtained, and so the long-period ground motions can be predicted at the stations considering the site-specific amplification factors. In this study we develop empirical regression relations to spatially interpolate the amplification factors in order to predict long-period ground motions at any places in the Kanto basin, the Nobi basin, and the Osaka basin. In addition we put a theoretical interpretation on the empirical relations.

In previous attenuation relations for long-period ground motions, the depth of the seismic bedrock with S-wave velocity of around 3.0 km/s, the depth of the hard rock overlaid on the seismic bedrock, or the combination of one of them and Vs30 (the average S-wave velocity down to 30 meters) are used as parameters for the empirical relations of amplification factors. The reason why the depths were used is that the depth information is easier to obtain than the velocity structure information. In 2009, long-period ground motion maps and the three-dimensional velocity structure models were open in public by the Headquarters for Earthquake Research Promotion in ministry of education, culture, sports, science and technology, Japan. In this study we calculate the average propagation time Tz3.2 from the seismic bedrock with the S-wave velocity of 3.2 km/s to the engineering bedrock using the velocity structure models and develop empirical regression relations of amplification factors using Tz3.2.

It is found that the logarithm of the empirical amplification factors C are represented bi-linear-type regression lines with the connection Tz3.2 of 1 second in a period range from 0.5 to 10 seconds in three basins. The C is modeled by the equations (1) and (2).

$$\log_{10}C = a_1 + b_1 Tz_{3.2} \quad (Tz_{3.2} > 1.0) \quad (1)$$

$$\log_{10}C = a_2 + b_2 Tz_{3.2} \quad (Tz_{3.2} < 1.0) \quad (2)$$

Here a<sub>1</sub>, a<sub>2</sub>, b<sub>1</sub>, and b<sub>2</sub> are regression coefficients. The correlation between C and Tz<sub>3.2</sub> is better than that between C and the depth of the seismic bedrock. We simulate the C at eight stations in three basins using the regression relations and confirm that the regression relations reasonably represent the C by considering the standard deviations of the regression relations and the standard deviations of C.

Then we put a theoretical interpretation on the empirical relations of the amplification factors using medium responses. First, we calculate medium responses of the fundamental mode of the Love waves and Rayleigh waves from the velocity structures just beneath the observation stations using the three-dimensional structure models. Secondly, we get horizontal components of the Rayleigh waves multiplying the medium responses by horizontal-to-vertical spectral ratios of the Rayleigh waves. Then we add the medium responses of Love waves to them and define them as MR in this study. Finally we analyze the relation between MR and C at each period. It is found that the relation between Tz<sub>3.2</sub> and logarithm of MR is correlated well with the relation is between Tz<sub>3.2</sub> and logarithm of C. This results suggest that the empirical regression relations of the equations (1) and (2) have the theoretical basis.

**Acknowledgements:** The authors express their sincere thanks to the members of the Committee on the Study of the Long-Period Strong Motions and the Working Group on Strong Motions and Responses for their relevant ideas and suggestions. The financial support of the Japan Ministry of Land, Infrastructure, Transport and Tourism is also acknowledged.

**Keywords:** long-period ground motions, empirical attenuation relations, amplification factors, velocity structure model, medium response

SSS023-15

Room:IC

Time:May 23 12:15-12:30

## Evaluation of Site Effects for Acceleration Response Spectra based on Recorded Data

H. Serdar Kuyuk<sup>1\*</sup>, Hongjun Si<sup>1</sup>, Kazuki Koketsu<sup>1</sup>, Hiroe Miyake<sup>1</sup>

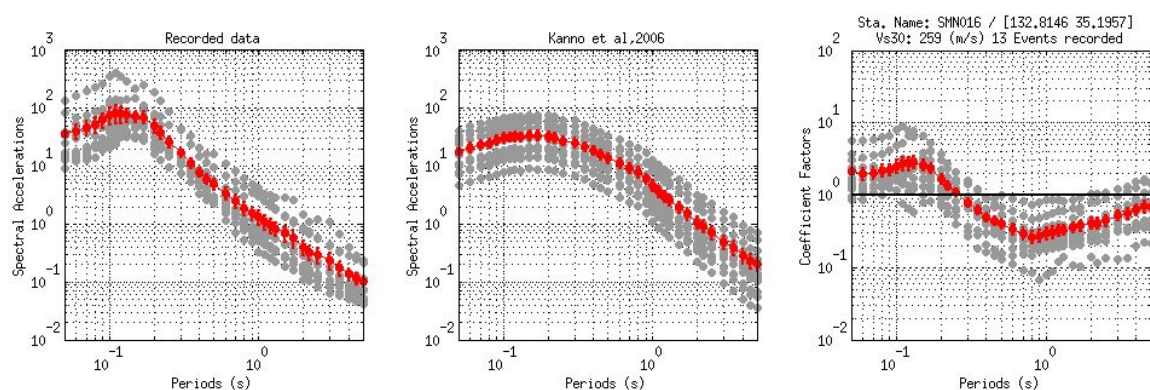
<sup>1</sup>Earthq. Res. Inst., Univ. Tokyo

Figure 1. a) Attenuation model for acceleration response spectra proposed by Kanno et al. b) acceleration response spectra using observed records c) site effect correction factors

Seismic networks, such as KIK-net and Hi-net, provide valuable information for studies in engineering and seismology. Research related to the site effect of strong ground motion attenuation use the soil information (especially those extracted from  $V_{s30}$ ) of the stations. Many other studies have been concerned with  $V_{s30}$  at K-NET stations assuming this is the parameter that correlates with site effect. On the other hand, some networks (more than 1000 locations) that are operated by JMA or local prefectural administrations do not have soil information. While  $V_{s30}$  is debated as the correct factor to evaluate site effects, Si et al, (2010) have proposed an effective yet easy methodology to assess site effect in attenuation relationships. This correction factor (CF) for site effect is not a function of  $V_{s30}$  but instead is dependent on previous recordings. It is calculated by employing an average operator of the ratio of observed ground motion to a reference attenuation model. The advantage of the method is that the site effect can be estimate without soil information.

Kanno et al, (2006) proposed a standard attenuation relation considering acceleration response spectra for Japan. They used a CF function of  $V_{s30}$  which were determined from KIK-net stations and summed these with spectral amplitudes in particular frequencies. They applied the CF to their data and were able to reduce the standard error. We use this attenuation relationship as a reference model in our analysis. The method was tested in an area bounded by 133-135E longitude to 32-36N latitude in which 152 K-NET stations are located. We focus on the Tottori region and have evaluated 46 crustal earthquakes with  $M_w > 4.0$ . From over 7000 records we extracted 596 records that satisfied two criteria a) the stations were within 100 km hypocentral distance and b) the recorded seismic signal was larger than 10 gal.

The acceleration response spectra calculated attenuation model by Kanno et al, (2006) is shown in Figure 1a. Here, the K-NET station SMN016 with a  $V_{s30}$  value of 259 m/s is given as an example. Figure 1b is acceleration response spectra estimated from 13 events recorded at that station from 1997 to 2010. The coefficient factors are plotted in Figure 1c. We observed that the method gave sufficiently good results if there are adequate station records. We find good agreement between our results and previously methods that use  $V_{s30}$ . Thus, the methodology used in this study is an alternative method for evaluating site effects to obtain more reliable attenuation relationship models.



Keywords: Site effects, acceleration response spectra, Tottori region



## An attempt to replicate the so called "trampoline effect" in computational geomechanics

Akira Asaoka<sup>1\*</sup>, Toshihiro Noda<sup>2</sup>, Shotaro Yamada<sup>2</sup>, Takaine Toshihiro<sup>3</sup>

<sup>1</sup>Association for the Development of Earth, <sup>2</sup>Nagoya University, <sup>3</sup>Asanuma co., ltd.

A loosely deposited alluvial sand subjected to a small seismic motion will initially pack together more firmly. But when a large shearing force is repeatedly brought to act on this well compacted soil, the sand will loosen up again and gradually start to swell. In the first stage of the research reported here, the SYS Cam-clay model proposed by the authors<sup>1)</sup> to represent the soil skeleton's elastoplastic constitutive equation is used to replicate a soil behavior of this kind. This model of the elastoplastic constitutive equation is arrived at by incorporating the evolution behaviors of three constituent conceptual of the soil skeleton (structure, overconsolidation, and anisotropy) into the Cam-clay model; the combined model is then capable of reproducing the mechanical behaviors of all soil types from sand to clay, including any intermediate types.

Keeping this representation of the soil skeleton behavior in mind, the present research goes beyond it in using the soil-water coupled finite deformation analysis code **GEOASIA**<sup>2)</sup>, created by mounting the SYS Cam-clay model onto the constitutive equation, to show what occurs when a ground in an overconsolidated state is subjected to an additional strong seismic motion; the soil becomes progressively looser, which may lead to swelling and rising in the ground. The **GEOASIA** analysis code makes it possible to carry out a time history analysis of the phenomena taking place in the ground and in the soil structures resting on it, not only for any kind of soil, but also without restriction for any mechanical states involved, stable or unstable, and over all ranges of instability, from deformation to failure, or liquefaction to subsequent reconsolidation in the case of sand. Similarly, the analysis performed can be static or dynamic, and provision can be made for any kind of external disruption affecting the ground. The analysis reported here concerns an event in which the ground resonates with the incoming seismic motion. The large shearing forces repeatedly acting on the soil elements are shown to induce loosening in the soil skeleton, which may result in local swelling and rising at the time of the earthquake. The analysis also shows that the input acceleration applied to the foundation (taken to mean the lower edge of the area analyzed) provokes vertical response movements at the surface, even when the acceleration wave consists only in a horizontal component. Further, it is found that the resultant acceleration wave has a very marked asymmetry in the vertical direction, whereas the waveform in the horizontal direction is symmetrical. This recalls the result of measurements obtained at the KiK-net seismograph station IWTH25 (West Ichinoseki) at the time of the 2008 Iwate-Miyagi earthquake, which indicated a similar powerful seismic motion with marked asymmetry in the vertical component only (Aoi et al., 2008<sup>3)</sup>). The peculiarities in the acceleration wave noted by these authors were a large upward pulse compared with a smaller downward one, the fact that downward acceleration appears to peak at around 1g, and the greater width of the waveform in its downward pulses than in its upward ones (Fig. 1). The given physical ground values, input seismic wave details, etc., required for the analysis are not based on the West Ichinoseki data, but nevertheless the distinctive nonlinear ground response measured there during the earthquake could also be confirmed in the results of the present analysis, using a continuum approximation to earth as an elastoplastic body (Fig. 2).

1) Asaoka, et al. (2002): An elasto-plastic description of two distinct volume change mechanisms of soils, *Soils and Foundations*, **42(5)**, 47-57.

2) Noda, et al. (2008): Soil-water coupled finite deformation analysis based on a rate-type equation of motion incorporating the SYS Cam-clay model, *Soils and Foundations*, **48(6)**, 771-790.

3) Aoi, et al. (2008): Trampoline effect in extreme ground motion, *Science*, **322**, 727-730.

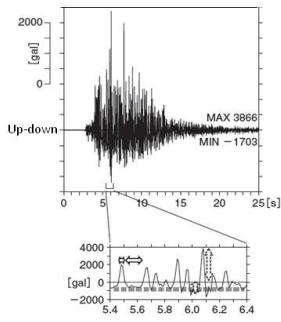


Fig. 1 Time history of ground surface acceleration response (observed results)<sup>3)</sup>

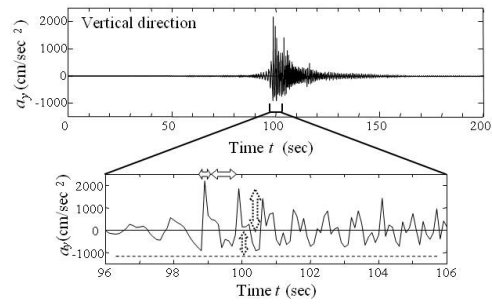


Fig. 2 Time history of ground surface acceleration response (analyzed results)

Keywords: strong motion earthquake, swelling/rising phenomenon, asymmetric waveform, elastoplastic constitutive equation, loosening, resonance

# Japan Geoscience Union Meeting 2011

(May 22-27 2011 at Makuhari, Chiba, Japan)

©2011. Japan Geoscience Union. All Rights Reserved.



SSS023-17

Room:IC

Time:May 23 14:15-14:30

## CMT inversion considering the isotropic component-Focal mechanism difference between a fault event and a volcanic one-

Takeshi Kurose<sup>1\*</sup>, Satoru Fujihara<sup>1</sup>, Shinichi Akiyama<sup>1</sup>, Hiroaki Yamanaka<sup>2</sup>

<sup>1</sup>ITOCHU Techno-Solutions Corp., <sup>2</sup>Tokyo Institute of Technology

In the CMT inversion of a fault-type event, it is commonly assumed that there is no contribution of the isotropic component. However, in the case of a volcanic event or an artificial one, it is considered that the isotropic component is not negligible. In this study, we develop a CMT inversion code considering the isotropic component, and investigate a focal mechanism difference between a fault-type event and a volcanic one by using the code.

Keywords: CMT inversion, isotropic component, fault-type earthquake, volcanic earthquake, focal mechanism, earthquake ground-motion characteristics

SSS023-18

Room:IC

Time:May 23 14:30-14:45

## Near-real-time imaging of earthquake rupture by normalized short-period envelopes

Shigeki Aoki<sup>1\*</sup>, Yasuhiro Yoshida<sup>1</sup>, Akio Katsumata<sup>1</sup>

<sup>1</sup>Meteorological Research Institute

### 1. Introduction

After a great earthquake, real-time estimations of rupture area and locations of asperities are important to assess hazards due to tsunami and ground shaking. However, it takes long time to analyze source process by the waveform inversion. Aoki et al. (2010, SSJ) developed a method for near-real-time imaging of earthquake rupture by normalized short-period envelopes, and succeeded in depicting rough image of rupture process of the 2003 Off Tokachi Eq. (TKEQ). In this study, we apply our method to the 1994 Far E off Sanriku Eq. (SREQ), and evaluate the accuracy for location and timing of the rupture.

### 2. Method

Our method is based on the Source-Scanning Algorithm [Kao & Shan, 2007]. It is applied for identifying the rupture plane. The brightness of a grid point is calculated by summing the amplitudes of normalized envelopes with the correction of the S-wave travel times at all stations. The grid points are arranged not on the prescribed fault plane, but in the 3D source volume. The composite image of the brightness of all grid points illuminates the locations and timings of seismic rupture (e.g. asperity). The normalized short-period (5-10Hz) envelopes give us an advantage of reducing the effect of site amplification factors, radiation patterns [Kamae et al., 1990] and surface waves [Izutani & Hirasawa, 1987]. In addition, our method is robust to outliers because the brightness is defined as the average amplitude of all stations, and is suitable for real-time processing.

### 3. Application to the SREQ

We used 17 JMA 87-type accelerometers within 500km from the epicenter. The grid points were arranged in and around the aftershock area (200km (NS) x 400km (EW) x 90km (depth)) at 2km interval. The brightness of each grid was calculated for 120 sec after the initial rupture.

The maximum of brightness (0.89) was appeared at 54s, and its location was 129km in N83W of the epicenter, and the depth was 26km. This point was close to the high frequency source [Sato et al. (1996), 51s, 137km in N82W, and 49km depth], except for the depth with low resolution. In the brightness snapshots from 27.5s to 63.0s, the peak brightnesses exceeded 0.7. The trace of the peak brightness almost corresponded to that of large slip area estimated by the waveform inversion [Nakayama & Takeo, 1997].

In this study, data length must be more than 5 minutes after the origin time, and it took about 15 minutes of calculation by an Intel Xeon X5550 (2.66GHz). For the TKEQ, the data length must be more than 3.5 minutes, and the computation time was about 4 minutes. To reduce the computation time, we plan to investigate the proper number of the grid points and to modify the code for parallel computing.

### 4. Discussion

The brightness image is interpreted as a superposition of a real rupture image and a blurring effect, which is due to a gap of station distribution, rupture duration and a wave scattering. In this section, we evaluate the blurring effect on the basis of the brightness images of point-source-like aftershocks and synthetic envelopes.

We estimated the M5.0 aftershock near the asperity of the TKEQ by the same station distribution as the main shock. The maximum was appeared at 1.0s, the location was 18km from the epicenter. In the case of the M5.6 aftershock of the SREQ, the peak was appeared at 5.0s, the location was 6km away. In both cases, the grid points having more than 0.7 in the brightness were distributed within 55km in horizontal distance, and ranged from -10s to 10s in time.

We compare the images calculated by the synthetic envelopes with and without scattering effect. The scattering effect is evaluated on the basis of the theory by Saito et al. (2002). Consequently, the image with scattering effect was more similar to that of the real aftershock. These results show that our method was influenced by scattering effect and the image was broadened.

Keywords: Near-real-time processing, Source process, The 1994 Far E Off Sanriku Earthquake

SSS023-19

Room:IC

Time:May 23 14:45-15:00

## Uncertainty of Kinematic Source Inversion Solution by Resampling Test in Case of the 2007 Noto Hanto Earthquake

Kimiyuki Asano<sup>1\*</sup>, Tomotaka Iwata<sup>1</sup>

<sup>1</sup>DPRI, Kyoto University

Kinematic source inversion using strong motion and GPS data gives detailed image of the heterogeneous source rupture process during large earthquakes. The obtained source models have been used to discuss the relationship between the heterogeneous rupture process and the near-source strong ground motions and to develop the strong motion prediction technique based on the recipe (e.g., Iwata, 2009). However, there are critical discussion on the stability and reliability of the kinematic source inversion results, and an international project for source inversion validation was launched (e.g., Mai *et al.*, 2010). In this study, we analyze the stability and uncertainty of the kinematic source inversion solution by bootstrap approach using the data set for the 2007 Noto Hanto earthquake.

As for the 2007 Noto Hanto earthquake, we have already obtained the source rupture process by the multiple time-window linear waveform inversion method (Hartzell and Heaton, 1983) using the velocity waveform data at 12 strong motion stations of K-NET and KiK-net (0.05-1 Hz) and the horizontal static offset measured at 19 GPS stations of GEONET (Asano and Iwata, 2007). The one-dimensional velocity structure models for strong motion stations were optimized by the aftershock's waveform modeling. The relative weight between strong motion and GPS data and the smoothing strength were objectively determined by minimizing ABIC.

In this study, we generated 1000 data sets by randomly removing three strong motion stations and four GPS stations from the original data set. From 1000 solutions, we calculated the averages, standard deviations, and the coefficients of variation of the total seismic moment and the slip amount at each subfault. The average total seismic moment is  $1.64 \times 10^{19}$  Nm and average maximum slip is 4.8 m, those are comparable to the estimation by Asano and Iwata (2007). Those coefficients of variation are 9% and 11%, respectively. We will also investigate spatiotemporal characteristics of those statistical parameters in detail. From above analyses, we can conclude that we could obtain the reliable stable solution if we used efficient number of data and appropriate velocity structure model.

Acknowledgments: Strong motion data of K-NET and KiK-net of NIED and the daily coordinate data of GEONET of GSI are used in this study.

Keywords: kinematic source inversion, uncertainty, strong motion data, GPS data, the 2007 Noto Hanto earthquake

# Japan Geoscience Union Meeting 2011

(May 22-27 2011 at Makuhari, Chiba, Japan)

©2011. Japan Geoscience Union. All Rights Reserved.



SSS023-20

Room:IC

Time:May 23 15:00-15:15

## Influence of super-shear on simulated near-source ground motion from the 1999 Izmit earthquake

Hideo Aochi<sup>1\*</sup>, Virginie Durand<sup>2</sup>, John Douglas<sup>1</sup>

<sup>1</sup>BRGM/RNSC, Orleans, France, <sup>2</sup>ISTerre, Grenoble, France

We numerically simulate seismic wave propagation from the 1999 Mw7.4 Izmit, Turkey, earthquake, using a 3D finite difference method based on published finite source models obtained by waveform inversions. This earthquake has been reported, based on observations at the near-fault station SKR, as an example of super-shear rupture propagation towards the east. Although the modeled ground motion does show a characteristic Mach wave from the fault plane, it is difficult to identify any particular effects in terms of peak ground velocity, an important parameter in earthquake engineering. This is because the fault spatial heterogeneity is strong enough to mask the properties of super-shear rupture, which has been reported through several numerical simulations mostly based on homogeneous fault conditions. This study demonstrates the importance of studying ground motions for known earthquakes through numerical simulations based on finite-fault source models.

Keywords: ground motion, super-shear rupture, Izmit earthquake, finite source models, finite difference simulation

SSS023-21

Room:IC

Time:May 23 15:15-15:30

## Strong motion simulation of the 2007/9/15 Peru earthquake; Effect of radiation pattern on atypical strong ground motions

Nelson Pulido<sup>1\*</sup>, Hernando Tavera<sup>2</sup>, Zenon Aguilar<sup>3</sup>, Shoichi Nakai<sup>4</sup>, Fumio Yamazaki<sup>4</sup>

<sup>1</sup>Nat. Res. Inst. Earth Sc. and Dis. Prev, <sup>2</sup>Instituto Geofisico del Peru, <sup>3</sup>Universidad Nacional de Ingenieria, <sup>4</sup>Chiba University

The 2007 Mw8.0 Pisco earthquake was a thrust event originating at the interface of the Nazca and South-American plates, in a region slightly north of where the Nazca ridge encounters the trench and is being subducted beneath the Peru margin. The source area of the Pisco earthquake was located 160 km south-east of Lima, off-shore of the Pisco city, in a region filling the gap between the 1974, Mw8.0 Lima earthquake, and the 1996, Mw7.7 Nazca ridge earthquake. The source model of this earthquake displays two distinct asperities, the first one located near the hypocenter at a depth of 39 km, and the second one located 60 km to the South at a depth of 17km (Sladen et al., JGR, 2010). The source time function of this earthquake was also characterized by two episodes of moment release, the first one at 10s and the second and largest one at 80s, separated by a very low apparent rupture velocity of 1.5 km/s. These features suggest that the earthquake may have been characterized by a delayed rupture of two isolated events, each with a conventional rupture velocity. Ground motions from this earthquake are also characterized by two clear sub-events originating from each asperity, as can be observed from strong motion recordings of the mainshock at Lima (NNA), and Parcona (PCN) stations. The acceleration waveform at PCN station, which is located above the source area of the earthquake, is characterized by an atypical pattern, namely that the peak amplitude corresponding to the first sub-event is more than 5 times larger than the peak amplitude from the second sub-event, despite the fact that the second sub-event has a much larger moment release and is located closer to PCN. To explain this unusual pattern one may think of large differences in the propagation characteristics between asperities 1, 2 and PCN, or differences originating at the source. We may rule out the contribution of site-effects to explain this difference as we can assume it is the same for both sub-events.

Based on the aforementioned source model we simulated the strong ground motions at PCN and compare it with the observed record. Our simulations show that a variable radiation pattern across the fault plane can provide an appropriate explanation on the relative differences in amplitude for the two sub-events at PCN. The radiation pattern of S waves for a point source at the centroid of asperity 2 shows that the location of station PCN is coincident with a nodal plane of SH waves. Therefore the large seismic radiation released from this asperity is dramatically reduced at PCN by a very small radiation pattern coefficient. In contrast the seismic radiation from asperity 1 is modulated by a large radiation pattern coefficient, as its azimuth relative to PCN differs by approximately 45 degrees with respect to the asperity 2 to PCN azimuth, thus enhancing the source contribution to amplitudes from the first sub-event at PCN. On the other hand the source model of the Pisco earthquake displays a small average rise time for asperity 1 (around 1s), as compared to a large rise time for asperity 2 (around 7s), which may also have contributed to magnify the amplitudes from asperity 1.

### Acknowledgements

This study is being conducted within the framework of a JICA/JST project entitled 'Enhancement of Earthquake and Tsunami Disaster Mitigation Technology in Peru'. The strong motion data at NNA and PCN stations belongs to the strong motion network of the Instituto Geofisico del Peru.

Keywords: 2007 Peru earthquake, Strong motion, radiation pattern, Nazca plate

SSS023-22

Room:IC

Time:May 23 15:30-15:45

## Strong motion simulation for the 2004 Chuetsu earthquake with special reference to large velocity at Ojiya

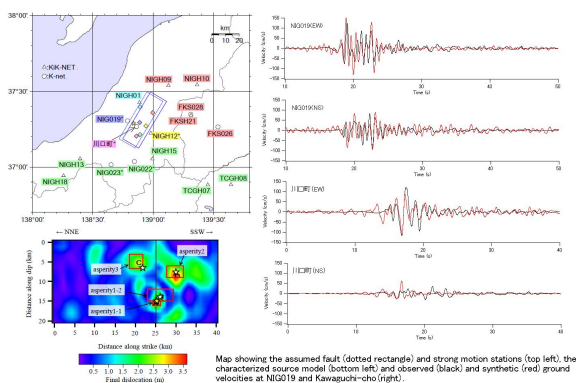
Atsushi Nozu<sup>1\*</sup>, Kimitoshi Sakai<sup>2</sup>

<sup>1</sup>Port and Airport Research Institute, <sup>2</sup>Railway Technical Research Institute

According to studies in the field of engineering seismology after the 1995 Hyogo-ken Nanbu earthquake, it was revealed that near-source velocity pulses can cause serious damage to structures (e.g., Kawase, 1998) and that these velocity pulses can be simulated using characterized source models quite accurately (e.g., Kamae and Irikura, 1998). These were the pulses that resulted from forward directivity effects. Since then, however, there have been many cases in which large amplitude (about 100 cm/s or more) ground velocities, which cannot be attributed to forward directivity effects, were observed in the near-source region of large crustal earthquakes in Japan. The strong ground motion observed at Ojiya during the 2004 Chuetsu earthquake is one of the examples. It is important from engineering point of view to investigate the validity of characterized source models for these cases.

For the 2004 Chuetsu earthquake, there have been several trials to construct characterized source models (e.g., Kamae et al., 2005) but none of them seemed to be quite successful in reproducing ground velocities including those at K-NET Ojiya and Kawaguchi-cho. In this study, the authors propose a new characterized source model, which is capable of reproducing near-source ground velocities including those at K-NET Ojiya and Kawaguchi-cho.

Empirical site amplification and phase characteristics were considered (Kowada *et al.*, 1998; Nozu *et al.*, 2009) in the simulation. There were two key factors that contributed to the reproduction of strong ground motions at K-NET ojiya in this study. One of them was selecting appropriate aftershock records to take into account phase characteristics. The other was taking into account nonlinear site response at K-NET Ojiya as revealed by Tokimatsu *et al.* (2006) and Tokimatsu and Sekiguchi (2006).



Keywords: strong ground motion, characterized source model, site amplification factor, phase, nonlinearity, The 2004 Chuetsu earthquake



SSS023-23

Room:IC

Time:May 23 15:45-16:00

## Broadband Ground Motion Prediction for Miyagi-oki Earthquake Scenarios

Hiroe Miyake<sup>1\*</sup>, Kazuki Koketsu<sup>1</sup>, Tetsu Masuda<sup>1</sup>, Haruhiko Suzuki<sup>2</sup>, Yasuhiro Kaida<sup>2</sup>

<sup>1</sup>Earthq. Res. Inst., Univ. Tokyo, <sup>2</sup>OYO Corp.

The omega-squared source model with a single corner frequency is widely used in the earthquake source analyses and ground motion simulations. Recent studies show that the Brune stress drop of subduction-zone earthquakes is almost half of that for crustal earthquakes for a given magnitude. On the other hand, the empirical attenuation relations and spectral analyses of seismic source and ground motions support the fact that subduction-zone earthquakes provide 1-2 times of the short-period source spectral level for crustal earthquakes. To link long- and short-period source characteristics is a crucial issue to perform broadband ground motion simulations. This discrepancy may lead the source modeling with double corner frequencies [e.g., Atkinson, 1993]. We modeled the lower corner frequency corresponding to the size of asperities generating for long-period (> 2-5 s) ground motions by the deterministic approach and the higher corner frequency corresponding to the size of strong motion generation area for short-period ground motions by the semi-empirical approach. We propose that the double corner source spectral model is expressed as a period-dependent source model consists of either the asperities in a long-period range or the strong motion generation area in a short-period range and the surrounding background area inside the total rupture area. The characterized source model has been the potential to reproduce fairly well the rupture directivity pulses seen in the observed ground motions. We explore the applicability of the double corner source spectral model to broadband ground motion simulations for the Mw 7.6 and Mw 7.3 Miyagi-oki earthquake scenarios along the Japan Trench. The Mw 7.6 scenario is similar to the source model of the 1978 Miyagi-oki earthquake. The double corner source spectral model, where the size and stress drop for strong motion generation areas are respectively half and double of those for asperities, worked well to reproduce broadband ground motion time histories and seismic intensity distribution of the 1978 Miyagi-oki earthquake.

This research was supported by the Integrated Research Project for Miyagi-oki Earthquakes from the Ministry of Education, Culture, Sports, Science and Technology (MEXT), Japan.

Keywords: broadband ground motion simulation, Miyagi-oki earthquake, characterized source model, Japan integrated velocity structure model, hybrid method

SSS023-24

Room:IC

Time:May 23 16:00-16:15

## Study on New Recipe for Predicting Strong Ground Motions from Intra-slab Earthquakes

Toru Ishii<sup>1\*</sup>, Satoko Murotani<sup>2</sup>, Sadayuki Kitagawa<sup>1</sup>, Kojiro Irikura<sup>3</sup>

<sup>1</sup>MEXT, Japan, <sup>2</sup>ERI, Univ. of Tokyo, <sup>3</sup>Aichi Institute of Technology

The Headquarters for Earthquake Research Promotion (HERP) have been making the long-term evaluation reports for inland crustal earthquakes along the major active faults and the major subduction-zone earthquakes which will occur in and around Japan in the future, and established the procedure to predict strong ground motions for scenario earthquakes, which has been named the Recipe. The objective of this study is to establish a new Recipe for intra-slab earthquakes.

Though both of inter-plate and intra-slab earthquakes belong to subduction-zone earthquakes, the present Recipe by HERP for subduction-zone earthquakes is fundamentally the one for inter-plate earthquakes. As for intra-slab earthquakes, few historical earthquakes have been observed, few data and knowledge have been obtained, and their characteristics have not been clarified enough. However in the last decade, some intra-slab earthquakes occurred, new knowledge was obtained from new data, and it is becoming necessary to consider the knowledge into the earthquake resistant design of important structures. Therefore, the Subcommittee for Evaluation of Strong Ground Motion of HERP has started studies to establish a new Recipe for intra-slab earthquakes.

Recently, procedures to make characteristic fault models of earthquakes were newly proposed, for example, Dan et al.(2006), Sasatani et al.(2006), Iwata and Asano(2010). Compared with inter-plate earthquakes, an intra-slab earthquake generates much more short-period seismic waves from its asperity with smaller size. Such characteristics of intra-slab earthquakes are important for the earthquake resistant design of short-period structures. Especially, Dan et al.(2006) and Sasatani et al.(2006) applied the empirical Green's function method to the strong ground motion records from recent intra-slab earthquakes, and presented empirical relations between the combined area of asperities and the seismic moment, empirical relations between the short-period source spectra level and the seismic moment, respectively. In this study, a new Recipe for intra-slab earthquakes is proposed, focusing on the asperity area and the short-period source spectra level, which are evaluated by using the above mentioned empirical relations. Firstly, the asperity area and the short-period source spectra level are evaluated from the assumed seismic moment. Then the effective stress on the asperity and the average static stress-drop on the entire fault plane are evaluated theoretically. The inner and outer source parameters are calculated successively by using empirical and theoretical relations.

Keywords: subduction-zone earthquake, intra-slab earthquake, strong motion prediction, recipe, fault model, asperity

SSS023-P01

Room:Convention Hall

Time:May 24 16:15-18:45

## Improvement of web interface of the IISEE earthquake catalog

Tatsuhiko Hara<sup>1\*</sup>, Toshiaki Yokoi<sup>1</sup>

<sup>1</sup>IISEE, BRI

We introduce recent developments of the web interface of the IISEE (International Institute of Seismology and Earthquake Engineering) earthquake catalog, "IISEE's CMTs, Aftershock Distributions, Fault planes, and Rupture processes for recent large earthquakes in the world" ([http://iisee.kenken.go.jp/eqcat/Top\\_page\\_en.htm](http://iisee.kenken.go.jp/eqcat/Top_page_en.htm)). In this catalog, we have been providing earthquake information (CMT, aftershock distribution, fault plane, and rupture process) determined by the analytical techniques developed by the IISEE and visiting researchers since 2008.

We have modified the top of the search page of this catalog so that registered events are shown on the Google Map. Users can select an event on the Google Map, and display earthquake information for that event in another window. In the web interface, we have implemented a function to forward earthquake information to web calculators of PGA, PGV, intensities, etc. using a set of attenuation equations. Calculation results are shown on maps drawn by the GMT (Generic Mapping Tools, Wessel and Smith, 1998). Earthquake source parameters for this calculation can be changed by users for their purposes and conditions such as soil, earthquake type, etc. This improved web interface is now available at our web site as a test version ([http://iisee.kenken.go.jp/cgi-bin/eqcatalog.newv4/eqcatalog2\\_eng.cgi](http://iisee.kenken.go.jp/cgi-bin/eqcatalog.newv4/eqcatalog2_eng.cgi)). We plan to implement a function to download calculation results using attenuation equations. Through these developments, we are improving combination among this earthquake catalog, strong motion calculations, and the other earthquake catalog available at our web site, "Catalog of Damaging Earthquakes in the World" (Utsu, 2004). The later updates are added by the IISEE).

Keywords: earthquake catalog, attenuation equation, web interface

# Japan Geoscience Union Meeting 2011

(May 22-27 2011 at Makuhari, Chiba, Japan)

©2011. Japan Geoscience Union. All Rights Reserved.



SSS023-P02

Room:Convention Hall

Time:May 24 16:15-18:45

## A feasibility study of fast and continuous strong-motion observation

Takashi Kunugi<sup>1\*</sup>, Hiromitsu Nakamura<sup>1</sup>, Shin Aoi<sup>1</sup>, Shohei Naito<sup>1</sup>, Shigeki Adachi<sup>1</sup>, Hiroyuki Fujiwara<sup>1</sup>

<sup>1</sup>NIED

Most earthquake early warning systems including JMA EEW predicts strong-motion parameters (seismic intensity, PGA) using estimated earthquake parameters (epicenter location, focal depth, magnitude) and attenuation equation. Thus, prediction of strong-motion parameter is affected by estimation error of earthquake parameters and inaccuracy of attenuation equation. We can, however, observe the true value of strong motion parameter at each observation site where main part of ground motion has arrived in a certain time after the earthquake occurrence. We can improve accuracy of prediction of strong-motion parameters using observed value of strong-motion parameters if strong-motion data is available in real-time. For this purpose and also real time seismic risk evaluation, National Research Institute for Earth Science and Disaster Prevention (NIED) started research and development of the real-time strong-motion monitoring system. One of the key components of the system is fast and continuous strong-motion observation.

We studied for feasibility of fast and continuous strong-motion observation using tens of K-NET strong-motion seismographs in operation. We installed an improved firmware in K-NET seismograph. The firmware can continuously send waveform data in 0.1s-length packet. Investigating packets sent by 35 K-NET seismographs in 38 hours through 64kbps best-effort type communication line, we concluded the end-to-end packet delay of most packets are shorter than 0.2s. Time delay of 0.2s is acceptable for our use.

Keywords: strong-motion observation, strong-motion seismograph, earthquake early warning

SSS023-P03

Room:Convention Hall

Time:May 24 16:15-18:45

## A New Method to Extract Building Response Parameters from Microtremor Data

Xin Wang<sup>1\*</sup>, Kojiro Irikura<sup>1</sup>, Kazuaki Masaki<sup>1</sup>

<sup>1</sup>Aichi Institute of Technology

Generally, a building can be considered as a system which is composed of the upper structure, the base, and the supporting ground of the building. Therefore, the response of a building system can be seen as a composition of the response of the upper building (fixed-base building) and the response of rigid-body due to the soil-structure interaction including rocking and horizontal vibration (sway). In order to fulfill the building damage analysis meticulously, extracting the response parameters of (A) the building system, (B) the fixed-base building, and (C) the soil-structure interaction from ground motion records of buildings is very necessary. There have been proposed many methods to extract the building response parameters (A)-(C) respectively. The methods so far used need to have many observation points on the first and top floors. We proposed a simple and easy method to extract all of the building response parameters (A)-(C) from the fewest points, one on the first floor and one on the top of the building. Microtremor records are often used to extract building response parameters, because they can be easily obtained at any time.

The new method to extract the building response parameters (A)-(C) from microtremor records of the 1F and the top of the building is presented based on the Deconvolution method, which was proposed by Snieder and Afak (2006) based on the interferometry method and was improved by Todorovska (2009a, 2009b). It is a very good method to extract the response parameters of fixed-base buildings and the base rocking vibration. The feasibility of this method to extract the response parameters from observed records on buildings during earthquakes has already been proved by the proposers. Based on the deconvolution method, in this paper, a method to extract the response frequencies of the building system ( $f_b$ ), the fixed-base building ( $f_{fb}$ ), rigid-body rocking ( $f_r$ ), and rigid-body sway ( $f_s$ ) from microtremor records on the top and the base of buildings is proposed. The feasibility of our method is examined by comparing the extracted building response parameters from microtremor data recorded on a 6-story building (Building No.2 in the Yakusa campus of the Aichi Institute of Technology) with those extracted from earthquake records on the same building and the numerical analysis results obtained based on the multi-degree-of-freedom model of this building. This method not only makes the extraction of building response parameters easier using only the records of the base and the top floor of buildings, but also provides an approach to extract the S-wave velocity traveling within the buildings using the records of the inter floors.

Keywords: Microtremor, Response Parameters, Deconvolution Method, Damage Level, S-wave Velocity

SSS023-P04

Room:Convention Hall

Time:May 24 16:15-18:45

## Multiple, Three-Dimensional Interactions between the Ground and a Group of Structures Subjected to Seismic Impact

Koji Uenishi<sup>1\*</sup>, Ioan R. Ionescu<sup>2</sup>

<sup>1</sup>Res Ctr Urb Safety & Security, Kobe Univ, <sup>2</sup>LPMTM, University of Paris 13

In our earlier study, using a fully coupled, two-dimensional ground-structure model, we have investigated the dynamic interactions between a set of identical buildings in a town and shown the collective behavior of the buildings during a seismic excitation: Due to the multiple interactions through (the waves in) the ground, the eigenfrequencies of the collective building system, i.e., town, become lower than the resonant frequency of a single building. This shift of eigenfrequencies may be called the "town effect" (or "city effect"). Our analysis is different from the conventional ones where each structure is handled individually, and the frequency shifts and "unexpected" structural behavior may be recognized only if the mechanical movement of the structural group is analyzed jointly. In the study, however, we have just considered the anti-plane shearing of a linear elastic half space on which identical buildings, each consisting of an elastic spring that connects a concentrated mass at the top and the rigid foundation at the bottom, stand. In this contribution, we shall briefly summarize some quantitative information about the two-dimensional anti-plane town effect and show its significance by investigating the actual structural damage patterns found on the occasions of several earthquakes in Europe and Japan. Then, we shall further consider the in-plane and three-dimensional cases and generalize the mathematical statement of the related problems. Since the "town effect" may be induced by dynamic structural impact in general (e.g., blasting), the simple analytical models handled here may contain the essential features that will play an important role in evaluating the dynamic performance of a group of structures in urban environments around the world.

Keywords: earthquake hazard, collective behavior, city effect, town effect, dynamic ground-structure interaction

# Japan Geoscience Union Meeting 2011

(May 22-27 2011 at Makuhari, Chiba, Japan)

©2011. Japan Geoscience Union. All Rights Reserved.



SSS023-P05

Room:Convention Hall

Time:May 24 16:15-18:45

## Seismic intensity of the two earthquakes (Dec.17-18,2009) off the east Izu Peninsula, based on a questionnaire survey

Masaki Mochizuki<sup>1\*</sup>, Masato Koyama<sup>2</sup>, Yoshinari Hayashi<sup>3</sup>

<sup>1</sup>Faculty of Education,Shizuoka University, <sup>2</sup>CIREN,Shizuoka University, <sup>3</sup>Faculty of Safety Science,Kansai Univ.

A questionnaire survey was made to clarify the detailed distribution of seismic intensities of the two largest earthquakes (M5.0 and M5.1 on December 17-18, 2009), which were associated with the earthquake swarm off the east coast of the Izu Peninsula, Japan. We distributed questionnaire sheets, which were based on the method by Ota et al. (1998), to 10 elementary schools in Ito City and requested them to be answered by all the households of their schoolchildren. In addition, we made the same surveys on the households lived in the middle parts of Ito City (Nagamiyo, Komuro-iccho, Komuro-nichome, and Joboshi areas), where severe damages were reported. 2557 available answers were collected and converted to JMA seismic intensity at each locality. These intensities were mapped and compared with topographic and geologic maps. While the mean intensity in Ohara shows 4.6 (5 lower in JMA scale), which is the same as that measured by a seismic intensity meter, the intensities at many points in Nagamiyo and Komuro-iccho show 6 lower and the mean value is 5.4 (5 upper). The mean intensity (5 lower) in Komuro-nichome is the lowest in the above four sections. This was probably caused by the hard basement, that is composed of thick lava flows from Komuroyama Volcano.

SSS023-P06

Room:Convention Hall

Time:May 24 16:15-18:45

## Examination of construction methodology of source model in case of multi-segment rupture

Masayuki Kuriyama<sup>1\*</sup>, Hiroaki Sato<sup>1</sup>

<sup>1</sup>CRIEPI

Investigating a fault model of the 1891 Nobi earthquake, which is one of the multi-segment rupture events, is significant for the establishment of source model construction methodology for strong ground-motion prediction. In Kuriyama and Sato (2010), we measured microtremors in the heavily damaged region caused by the Nobi earthquake to examine the relationship between seismic intensities, the ratio of the damaged houses, and the predominant period of H/V spectral ratio. We estimated the distribution map of seismic intensities by considering the local site effect of surface geology based on the above mentioned relationship. From these results, we found that the microtremor-measurement stations with questionnaire-based intensity of 7 in the Nobi Plain are almost linearly distributed only along the northern part of the Gifu-Ichinomiya Line (hereafter, GI Line) of the Research Group for Active Fault of Japan (1991). In this study, we conduct strong ground-motion simulations of the 1891 Nobi earthquake for three multi-segment rupture cases: (1) including the GI Line, (2) omitting the GI Line, and (3) including northern part of the GI Line.

For strong ground motion simulations, we construct three characterized source models (Irikura and Miyake, 2001). This type of model is one of the most reliable approaches for broadband strong ground-motion prediction. We conduct strong ground-motion simulations using the stochastic Green's function method for each third area mesh in the Nobi Plain. The horizontal acceleration waveforms are simulated on the seismic bedrock to examine the effect of the causative faults on the generation of the destructive ground motion. Here, we use the subsurface structure model of the Chukyo area of Horikawa et al. (2008). Based on the distribution of the simulated seismic intensities, we discuss the fault model of the Nobi earthquake.

Here, we compare the distribution pattern of simulated seismic intensities on the seismic bedrock in each case with that of estimated seismic intensities by considering the local site effect of surface geology in Kuriyama and Sato (2010). We could not find the linear distribution of larger seismic intensities that were present in Kuriyama and Sato (2010) along the GI Line from the distribution of simulated seismic intensities on the seismic bedrock in the multi-segment rupture case omitting the GI Line. In the case including the GI Line, the simulated seismic intensities along the southern part of the GI Line are slightly larger than expected. Meanwhile, the distribution of simulated seismic intensity in the case including the northern part of the GI Line is similar to the distribution map of Kuriyama and Sato (2010). We will conduct strong ground motion simulations on the engineering bedrock in the Nobi Plain and discuss the fault model of the Nobi earthquake.

Acknowledgement: The subsurface structure model of the Chukyo area of Horikawa et al. (2008) is used in this study.

Keywords: The 1891 Nobi earthquake, Predominant period of H/V spectral ratio of microtremors, Questionnaire-based intensity, Strong ground motion simulation, Source-model construction methodology



SSS023-P07

Room:Convention Hall

Time:May 24 16:15-18:45

## Broadband ground motion simulation for great earthquakes along Sagami Trough

Haruko Sekiguchi<sup>1\*</sup>, Masayuki Yoshimi<sup>2</sup>, Haruo Horikawa<sup>2</sup>

<sup>1</sup>DPRI, Kyoto University, <sup>2</sup>AFERC GSJ/AIST

Possible scenarios of great earthquakes along Sagami trough are modeled combining characteristic properties of the source area and adequate variation in source parameters in order to evaluate possible ground motion variation due to next Kanto earthquake.

We assume the rupture area of 1703 Genroku Kanto earthquake as the possible largest rupture area which consists of three fault segments. On the segment which also ruptured during the 1923 Taisho Kanto earthquake, we assume two sticking asperities which are derived commonly among source inversion analyses of this earthquake.

We construct many earthquake scenarios varying extent of the rupture area, the average stress drop, the average rupture velocity, hypocenter location and random heterogeneity of the source parameters with scale smaller than asperities. Variations of the average stress drop and the average rupture velocity are estimated from the variations of these values among the source models of past earthquakes.

The ground motions are computed with a four-step hybrid technique. We first calculate low-frequency ground motions at the engineering basement, which in this study is taken to be the depth at which the S-wave velocity exceeds 0.5 km/s. We then calculate higher-frequency ground motions at the same position, and combine the lower- and higher-frequency motions using a matched filter. We finally calculate ground motions at the surface by computing the response of the alluvium-diluvium layers to the combined motions at the engineering basement.

A comparison of ground motion distributions in the Kanto basin from the various earthquake scenarios suggests that source parameters which largely change the ground motion level in the wide are relocation of hypocenter and the average stress drop.

Keywords: ground motion prediction, Kanto earthquake, interplate earthquake, asperity, variation of parameter

SSS023-P08

Room:Convention Hall

Time:May 24 16:15-18:45

## Feasibility of near-real-time imaging of the rupture of megathrust earthquakes by normalized short-period envelopes

Shigeki Aoki<sup>1\*</sup>, Yasuhiro Yoshida<sup>1</sup>, Akio Katsumata<sup>1</sup>

<sup>1</sup>Meteorological Research Institute

### 1. Introduction

After a great earthquake, real-time estimations of rupture area and locations of asperities are important to assess hazards due to tsunami and ground shaking. However, it takes long time to analyze source process by the waveform inversion. Aoki et al. (2010, 2011) developed a method for near-real-time imaging of earthquake rupture by normalized short-period envelopes, and succeeded in depicting rough image of rupture processes of the 2003 Off Tokachi Eq. and the 1994 Far E off Sanriku Eq.

When Tonankai and Nankai Eqs. occur simultaneously in near future, the fault length will be 500km long, and the magnitude will be about M8.5 [ERC, 2001]. The megathrust earthquakes would have a lot of asperities on the fault. It is supposed that the rupture will start at off the Kii peninsula and will propagate bilaterally. We have applied our method to the earthquakes of M8.0 or smaller with unilateral rupture. Thus it is very important for us to evaluate the applicability of the method to a great earthquake with complex ruptures. In this study, we discuss the resolving power and application technique based on the simulated envelopes of the presumed Tonankai and Nankai Eqs.

### 2. Method

Our method is based on the Source-Scanning Algorithm [Kao & Shan, 2007]. It is applied for identifying the rupture plane. The brightness of a grid point is calculated by summing the amplitudes of normalized short-period envelopes with the correction of the S-wave travel times at all stations. The grid points are arranged not on the prescribed fault plane, but in the 3D source volume. The composite image of the brightness at all grid points illuminates the locations and timings of seismic rupture (e.g. asperity).

We used fixed stations to image the brightness for all grid points because the analyzed earthquakes had the fault length no more than 150km. However, in the case of the Tonankai and Nankai Eqs., the capability of our method is still unknown. In this study, we compare two cases. Case 1: imaging all grid points with the all stations. Case 2: dividing the grid points into some local sub-volumes, and imaging grid points in a sub-volume with limited stations near the sub-volume.

A simulated envelope was calculated by convolving the time series of the energy radiations with a synthetic envelope on the basis of the scattering theory including the effect of intrinsic absorption [Saito et al., 2002, 2005]. The energy radiation was estimated on the basis of the distribution of 9 asperities by the CDPC (2005).

### 3. Feasibility study for the Tonankai and Nankai Eqs.

In the case 1, the grid points were arranged in and around the presumed focal region (1000km (along the trough axis) x 200km (orthogonal to the axis) x 95km (depth)) at 4km interval. In the case 2, we divided the volume of the case 1 into 9 sub-volumes (200km x 200km x 95km) with an overlap of 100km along the axis. The brightness of each grid was calculated for 180 sec after the initial rupture. Simulated envelopes were evaluated at the locations of the JMA inland accelerometers and the cable-type OBSs installed by the JMA and JAMSTEC.

In the case 1, we used 84 stations within 500km from the epicenter. Consequently, we can roughly image only the nearest asperity from the epicenter in the side of Tonankai area, and cannot image the other asperities as the peak of the brightness more than 0.7.

In the case 2, we used 20 to 37 stations within 250km from a reference point in each sub-volume. As a result, we can image 7 asperities as the neighboring peaks of the brightness with 0.7 or greater. The two smallest asperities cannot be depicted. Though the ghost peaks tend to appear in the edge of the sub-volume, we can evaluate the reliance of the image due to the overlap of the sub-volumes.

We conclude that the case 2 is preferable for great earthquakes with complex ruptures. We plan to investigate the proper volume of the grid points for suppressing the ghost image and getting high resolution.

Keywords: Near-real-time processing, Source process, Simulation, The Tonankai and Nankai Earthquakes

SSS023-P09

Room:Convention Hall

Time:May 24 16:15-18:45

## Source inversion using curved fault model: Application to the two intraslab earthquakes in northeast Japan

Wataru Suzuki<sup>1\*</sup>, Shin Aoi<sup>1</sup>, Haruko Sekiguchi<sup>2</sup>

<sup>1</sup>NIED, <sup>2</sup>DPRI, Kyoto Univ./NIED

We have developed a new source inversion method using a curved fault model. The curved surface is constructed from the interpolation using Non-Uniform Rational B-Spline (NURBS). The multi-time-window linear waveform inversion method is implemented to the curved fault model. Applicability and effectiveness of the developed method are examined by applying the method to the two intraslab earthquakes that occurred in northeast Japan, the 2003 Miyagi-oki and 2008 northern Iwate earthquakes. They are considered to have the complex fault geometry from the source inversion analysis using strong-motion records (Wu and Takeo, 2004; Aoi et al., 2005; Suzuki et al., 2009). The waveform records of these earthquakes do not much suffer from the secondary generated seismic waves and clearly reflect the change of source mechanisms during the earthquake.

The slip distribution derived using the curved fault model shows that a large slip extends to an area that is a gap for a two rectangle fault plane model for the 2008 northern Iwate earthquake. This indicates that the curved fault, which would approximate the fault geometry more appropriately, could illuminate the slip that cannot be modeled by the planar fault model. The curved fault model gives the seismic moment closer to that derived from the moment tensor inversion than the two rectangular fault model. The moment tensor calculated from the slip distribution still differs from that derived from the moment tensor inversion. We will further investigate more appropriate fault model, which could give the moment tensor closer to the moment tensor solution. In the analysis of the 2003 Miyagi-oki earthquake, we can use the information of the aftershock distribution as well as the source mechanism and waveform fittings to construct the curved fault model. After we obtain the most appropriate fault model referring to the moment tensor calculated from the slip distribution and to the comparison of the waveforms, we will examine the effectiveness of the developed method compared with the inversion result using the rectangular fault model, particularly focusing on the extent of the asperities and the distribution of the stress change.

Keywords: source inversion, curved fault, strong motion, intraslab earthquake

SSS023-P10

Room:Convention Hall

Time:May 24 16:15-18:45

## Improvement of Source model for simulating strong ground motions during the 2008 Wenchuan earthquake

Susumu Kurahashi<sup>1\*</sup>, Irikura Kojiro<sup>1</sup>

<sup>1</sup>Aichi Institute of Tecnology

### 1. Introduction

The Wenchuan earthquake with a moment magnitude of 7.9 (United Statue Geological Survey,USGS) struck the western part of Sichuan Province on 14 May 2008, China, resulting in about 70,000 fatalities as well as huge damage to infrastructures and buildings. Causes of serious damage of structures should be attributed to characteristics of strong ground motions and vulnerability of structures.

The strong motion records during the Wenchuan earthquake will be very useful not only in making source modeling for estimating strong ground motion but also in clarifying the relation between structural damage and strong ground motions through reproduction of ground motions at damage sites. We estimated the characterized source model for simulating ground motions using the empirical Green's function (EGF) method and the hybrid method for the 2008 Wenchuan earthquake (Kurahashi and Irikura,2010). However, it has some problems. One of the problems is that the ground motions at Wolong station (WCW) in backward direction to Asperity 2 have smaller amplitudes, compared with the observed. Second, the contribution from asperities on the north-east segment to ground motions was not considered. In this study, to improve these two problems, the analysis was performed by the discrete wave number method. This model is a tentative version.

### 2. Analysis

We adopt basically the characteristic source model for the south-west segment reported by Kurahashi and Irikura (2010). The best model was determined by try and error. We used the observed records at 13 stations including the WCW, SFB and MZQ near the source fault. We find that the observed records at WCW are reproduced considering the rupture starting point of Asperity 2 not at the edge of the asperity area but inside it. This means that the rupture on Asperity 2 propagated not uni-laterally but bi-laterally. As a result, the area of Asperity 2 became larger of fit the observed records in forward direction such as SFB and MZQ as well as those in backward direction such as WCW.

Next, we estimated the contributions of asperities on the north-east segment to ground motions as stations in north-east direction.

There are several observation stations near the northeast segment. Remarkable wave pulses at the stations were not observed.

In this study, the best model was determined by try and error comparing the observed and the calculated motions. As a result, we presumed four asperities at the north-east segment. The stress drops on asperities are taken from 10 to 13 MPa. In future, we attempt to simulate ground motions using the empirical Green's function method.

SSS023-P11

Room:Convention Hall

Time:May 24 16:15-18:45

## Simulation of Strong Ground Motions during the 2009 Suruga-bay Earthquake using Empirical Green's Function and 3D-FEM

Koichiro Saguchi<sup>1\*</sup>, Susumu Kurahashi<sup>2</sup>, Kazuaki Masaki<sup>2</sup>, Kojiro Irikura<sup>2</sup>

<sup>1</sup>Nihon Emsco Ltd., Co., <sup>2</sup>Aichi Institute of Technology

Strong ground motions during the Suruga-bay earthquake occurring on August 11, 2009, were observed in the Hamaoka Nuclear Power Plant. The maximum acceleration on the basement of unit No. 5 reactor twice bigger than other sites was obtained during the main shock. In this study, we tried to simulate the strong ground motions of observation sites in the Hamaoka Nuclear Power Plant during the main shock using the hybrid method of the empirical Green's function method and the 3-D finite element method.

First, we tried to simulate strong ground motions at underground observation sites (3G1S) by the empirical Green's function method during the main shock. We selected an aftershock as the empirical Green's function for each segment of the source fault. For the asperity 1 and asperity 2, the observed records from an aftershock occurring at 12:42 on August 13, 2009 and those from another aftershock doing at 18:11 August 13, 2009 are used, respectively.

Next, strong ground motion in the seismic bedrock with  $V_s$  of 3.0km/s during the main shock was simulated considering 1-D velocity structure model.

Finally, strong ground motions at observation sites in the Hamaoka Nuclear Power Plant during the main shock were simulated using the three-dimensional finite element method considering three-dimensional velocity structure down to 10km, and input ground motion in the seismic bedrock mentioned above. The results indicate that the maximum accelerations in simulated waveforms were similar to the observed one.

Keywords: empirical Green's function method, 3-D finite element method, 2009 Suruga-bay earthquake, simulation of strong ground motions

SSS023-P12

Room:Convention Hall

Time:May 24 16:15-18:45

## Source process inversion of the 2007 Chuetsu-oki earthquake using theoretical 3-D Green's functions

Kazuhito Hikima<sup>1\*</sup>, Tomiichi Uetake<sup>1</sup>

<sup>1</sup>R & D Center, TEPCO

The strong motion waveforms are inverted for the source process of the 2007 Chuetsu-oki, Niigata, earthquake. One of the authors of this study has already performed the inversion analysis using theoretical Green's functions which are calculated with optimized 1-D horizontally stratified velocity models (Hikima and Koketsu, 2008). However, observed waveforms strongly suggest the existence of complex subsurface structures. Especially, the waveforms observed within the Kashiwazaki-Kariwa nuclear power station (KK NPS) are affected by fold structure beneath the KK NPS (Tokumitsu et al., 2009). So we have constructed 3-D velocity structure model and present the result at this meeting (Hayakawa et al., 2011). In this study, we calculate Green's functions for the source process analysis using this 3-D velocity structure and perform a inversion analysis.

Tentative analyses are preformed with same fault geometry and data set with Hikima and Koketsu (2008). We used 3-D Green's functions only for the stations in the KK NPS, because the 3-D model is not properly tuned in the area outside the KK NPS. So we used former 1-D Green's functions for the station except for the KK NPS. The inversion result is not so different with the result of Hikima and Koketsu (2008). However an asperity existing at the southern part on the fault plane moved toward the south and the coastline. Those results are consistent with other studies (ex. Shiba, 2008). However, time development on the fault is somewhat complex. We need detailed verification for the results.

Although the results have some problem, the observed waveforms in the KK NPS are well reproduced by the inversion analysis. Those results suggest that the fold structure beneath the KK NPS strongly affect the observed waveforms in the main shock of Chuetsu-oki earthquake.

Keywords: Chuetsu-oki earthquake, Source process, 3-D velocity structure, strong motion

SSS023-P13

Room:Convention Hall

Time:May 24 16:15-18:45

## Source model of the 2007 Chuetsu-oki earthquake based on precise aftershock distribution and 3-D velocity structure

Yoshiaki Shiba<sup>1\*</sup>, Kazuhito Hikima<sup>2</sup>, Tomiichi Uetake<sup>2</sup>, Hiroyuki Mizutani<sup>2</sup>, Kenichi Tsuda<sup>3</sup>, Takashi Hayakawa<sup>3</sup>, Shinya Tanaka<sup>4</sup>

<sup>1</sup>CRIEPI, <sup>2</sup>TEPCO, <sup>3</sup>ORI, <sup>4</sup>TEPSCO

In general it is necessary for a source inversion analysis to previously determine a fault plane model based on the focal mechanism and aftershock distribution. However, in case of the 2007 Niigata-ken Chuetsu-oki earthquake, the resolution of the aftershock distribution was rather low because of the source region lying offshore and the complex subsurface structure, hence the geometry of the main shock was difficult to determine. Precise aftershock distribution was eventually obtained using the records of the ocean bottom seismometers temporally installed on and around the source region after the main-shock occurrence, and it revealed a fault plane of the main shock dipping to the southeast (Shinohara et al., 2008). Moreover the detailed aftershock distribution shows a slight change in the alignment angle along the dip direction of the main shock, which suggests a distorted fault plane for the main shock. In this study we assume such a bending fault plane as an initial model for the source inversion analysis, and reconstruct the characterized source model for the broadband strong-motion simulation based on the inversion result.

The fault plane of the main shock is divided into three parts, which are the north, center, and south fault areas. The north and south faults are planar and only the central fault area implies a distorted plane. The dip angles for the north and south fault plane are assumed to be 40 and 30 degrees, respectively. The strike angle is 39 degrees throughout the whole fault. All the fault areas lie within the assumed seismogenic zone, the upper and lower limits of which are respectively 6 and 17 km. The length of the whole fault is assumed to be 28 km, being composed of 7 km for the north, 10 km for the center, and 11 km for the south fault area. The inversion analysis was carried out using the search method combining the empirical Green's function method and the simulated annealing, developed by Shiba and Iriguchi (2005). The estimated source model showed a similar slip distribution to the model obtained by Shiba (2008) assuming the totally planar fault plane, except for the location of the asperity close to the hypocenter, which slightly moves to the northwest. We further constructed the characterized source model that reproduces the strong-motion records observed at the base mats of the reactor buildings within the Kashiwazaki Kariwa nuclear power station (KK NPS). The optimal source model estimated by the forward modeling approach shows the 20% smaller in area and 10% lower in the stress drop for the asperity closest to the hypocenter, comparing with the previous model by Shiba (2008).

Furthermore, we attempt to simulate the distinct pulse waves observed at the KK NPS, showing obviously different amplitudes among the stations distributed within about 2 km. When the waveform-records of the aftershock occurring near the hypocenter of the main shock were used as the empirical Green's function, such variations of the pulse shapes among the observation stations could not be distinguished, probably due to inconsistent wave-propagating path with that from the southwestern asperity. In this study we employ the synthetic waveforms calculated by the finite difference method with the three-dimensional velocity model including fold structure beneath the KK NPS site (Hayakawa et al., 2011) and the observed records of the small aftershock of Mw 3.5, as the theoretical and empirical Green's functions. As a result the large pulse waveforms observed in the EW component at the KK NPS stations are successfully reproduced through the hybrid simulation.

**Acknowledgements:** We are grateful to Prof. Shinohara of ERI for providing us with the aftershock hypocenter data of the 2007 Chuetsu-oki earthquake based on the observation using ocean bottom seismometers.

**Keywords:** the 2007 Niigata-ken Chuetsu-oki earthquake, source model, aftershock distribution, 3-D velocity structure model, source inversion analysis, hybrid simulation

SSS023-P14

Room:Convention Hall

Time:May 24 16:15-18:45

## Modeling 3D Velocity Structure in the Fault Region of the 2007 Niigataken Chuetsu-oki Earthquake with Folding Structure

Takashi Hayakawa<sup>1\*</sup>, Kenichi Tsuda<sup>1</sup>, Tomiichi Uetake<sup>2</sup>, Kazuhito Hikima<sup>2</sup>, Ryoichi Tokumitsu<sup>2</sup>, Hideki Nagumo<sup>3</sup>

<sup>1</sup>OHSAKI RESEACH INSTITUTE, INC., <sup>2</sup>TOKYO ELECTRIC POWER COMPANY, <sup>3</sup>TOKYO ELECTRIC POWER SERVICES CO.,LTD.

### Introduction

The large ground motions were observed at the Kashiwazaki-Kariwa Nuclear Power Plant (KKNP) for the 2007 Niigataken Chuetsu-Oki earthquake (M6.8). This earthquake produced the large ground motion variations even in the narrow area such as inside the KKNP site. Previous studies, such as Tokumitsu et al. (2009), reported that this ground motion variation might come from the folding structure light below the site. This indicates that the folding structure is necessary to be considered for ground motion prediction. In this study, we have constructed the velocity model including the folding structure and validated it based on the simulation for moderate sized event.

### Construction of Velocity Model

The velocity model developed including broad Chuetsu area by Japan Nuclear Energy Safety Organization (JNES) (JNES, 2008) has been used as the basic model. The folding structure developed by Tokumitsu et al. (2009) is built into the broad model. We connected smoothly those two models to eliminate the artificial waves generated on the boundary area. We picked three events for the model validation. Two comes from the aftershocks of Chuetsu-Oki earthquake and the other comes from the aftershock of 2004 Chuetsu earthquake.

We could reproduce the general feature of ground motions at the KKNP site by the simulation for moderate sized events. The ground motion level was larger for south side of KKNP site than it for north side of KKNP site. These results suggest that the folding structure played an important role for ground motion during the main shock of Chuetsu-Oki event.

### Summary

We have constructed the velocity model including the folding structure. We could reproduce the general features of ground motion by the simulation for moderate sized events. The results of simulation indicate that the folding structure played an important role during the main shock of Chuetsu-Oki earthquake.

Keywords: 2007 Niigataken Chuetsu-oki Earthquake, Kashiwazaki-Kariwa Nuclear Power Plant, 3D velocity model, Fold, ground motion simulation



SSS023-P15

Room:Convention Hall

Time:May 24 16:15-18:45

## Three Dimensional Attenuation Structure beneath the Northern Kinki Region, Japan

Ryoichi Nakamura<sup>1\*</sup>, Kawasato Takeshi<sup>2</sup>

<sup>1</sup>Tokyo Electric Power Services Co.,Ltd., <sup>2</sup>The Japan Atomic Power Company

Spectrum inversions assuming uniform  $Q_s$  value (UQSI method) have been studied among many part of the country. Amaike et al.(2006) reported that the  $Q_s$  obtained using the UQSI method depend on data ranges on hypocentral distances and the  $Q_s$  decreases with the data ranges. Although, the causes of this phenomenon has not been cleared.

In this study, we obtained 3-D  $Q_s$  structure using 3-D  $Q_s$  spectrum inversion method (3DQSI method) with the discrete block size of 0.2 deg.\* 0.2 deg. \* 10 km and 0.2 deg.\* 0.2 deg. \* 20 km, and compared the 3-D  $Q_s$  results with  $Q_s$  by UQSI method reported by previous paper.

Data set are same as Nakamura et al.(2010), the 14,831 seismograms from K-NET and KiK-net from 1997 to 2007 that recorded 362 shallow and small earthquakes ( $h \leq 30$  km and  $4.0 \leq M \leq 6.0$ ) were used for tomography. The ground acceleration Fourier spectra for inversion were calculated by using the S-wave portion and taking the geometric mean of the spectrum within  $\pm 0.5$  Hz of central frequencies from 1 to 10 Hz every 1 Hz. The ground motion traces from the shallow earthquakes frequently have many later phases that consist of surface waves, therefore, the S-wave portion of records was selected to compare with the theoretical S-wave arrival time according to JMA2001. Other conditions for the tomographical calculations were in accordance with Nakamura(2009).

The Niigata-Ken Chuetsu area, Aichi-Gifu area and the northern Kinki region also show the good resolution in 1st layer (0-10 km in depth) and 2nd layer (10-20 km in depth). The active and quarternary volcanoes tend to show low- $Q_s$  at 0-10 km depth.

Fig.1 shows the relations between average  $Q_s$  and frequency obtained by taking the average  $Q_s$  over three study areas (A area:135.4-136.6 deg. E, 35.0-36.0 N, B area:135.2-136.2 E, 35.0-36.0 N, C area:135.4-136.6 E, 35.0-35.5 N) at layers 1 (0-10 km depth) and 2 (10-20 km depth).

Relation developed by Satoh et al. (2007) is also shown in this figure, they obtained  $Q_s = 50f^{1.1}$  by using the UQSI method and data of 60 km in hypocentral distance. The C area employs only good resolution blocks, and the A and B areas contain some blocks which are not good resolution.

Differences among these areas are small, and the results at the shallow layer (0-10 km depth) are in good agreement with Satoh et al. (2007).

Theoretical ray paths from sources at 10 km depth calculated using JMA velocity model shows only upward traveling to stations within about 60 km in epicentral distance, although in the case for the stations distant from epicenter, the rays travel downward once, and, next upward.

Satoh et al. (2007) used the data within 60 km on hypocentral distance. Therefore, the result,  $Q_s = 50f^{1.1}$ , mainly reflects  $Q_s$  of upper crust, and average  $Q_s$  at layer 1 (0-10 km depth) in this study agrees well with  $Q_s = 50f^{1.1}$ .

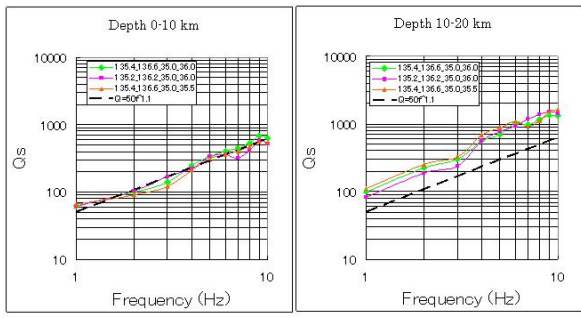


Fig.1 Comparison of  $Q_s$  values at the north Kinki region. Color solid lines: average  $Q_s$  by 3DQSI method (This study). Broken line:  $Q_s$  by UQSI method after Satoh et al (2007)

Keywords: 3-D attenuation structure,  $Q_s$ , spectral inversion, tomography, depth dependence, the Kinki region

## Characteristics of long-period ground motion in the Tokyo bay area

Sadanori Higashi<sup>1\*</sup>, Tomiichi Uetake<sup>2</sup>, Hiroaki Sato<sup>1</sup>

<sup>1</sup>CRIEPI, <sup>2</sup>TEPCO

It is well known that the long-period seismic ground motions at a period of several to more than a dozen seconds are predominant in the Kanto plain. We have compared the observation records of the broadband strong-motion seismometers installed in the thermal power plants in the Tokyo Bay area with the three-dimensional seismic simulations. We pointed out the possibility of the relation between the focal depth and the thick sedimentary basin in Sagami bay affects the later arrivals of the E-off Izu peninsula earthquakes with a magnitude of 5 occurred in 2006.

In this report the off Ibaraki Prefecture earthquake occurred on May 8, 2008 was used for investigating the characteristics of long-period seismic motions in the Kanto plain. We used an underground structure model with the range of longitude 138.2-142.0 degrees east and latitude 34.5-36.5 degrees north of the Headquarters for Earthquake Research Promotion (2009). We performed three-dimensional simulations by using a finite difference method with the grid point interval of 400m in horizontal direction and 100-400m in vertical direction. The duration of the calculated velocity waveforms are 300 seconds, which are 30,000 steps with an interval time of 0.01 seconds. We compared the waveforms with the velocity records at a frequency range of 0.08 to 0.12 Hz, which is 7 to 12 seconds in period.

We assumed two cases of the source models of the off Ibaraki Prefecture earthquake of 2008 as a point source. One is the deep source model at a depth of 50km derived from the JMA hypocentre with a F-net mechanism and the other is the shallow source model derived from JMA CMT mechanism at a depth of 28km. We also assumed two cases of the Q-values at each layers of the underground structure model. One is the original value of  $Q=Vs/5$  and the other is  $Q=Vs/2.5$ . We introduced the Grave(1996)'s Q-value model in the finite difference method and the reference frequency was 0.1Hz.

From the results of the comparisons between the two Q-value models with a deep hypocenter, no significant changes in amplitudes and later phases were seen in the frequency range of 0.08-0.12Hz. The calculated waveforms at IBR018 and IBRH20, which are the nearest the hypocentre, and from CHB004 to the observation stations in the eastern side of the Tokyo bay area are underestimated and are 1/3 to 1/4 in amplitude compared with the observed waveforms. Especially the later arrivals with large amplitude observed at the eastern bay area were not reproduced. On the other hand, the reproducibility at the western bay area is considerably better than the eastern area.

The results of the two kinds of different hypocenters showed great differences in amplitude and wave groups. It seems that the shallow case generally showed a better agreement with the observation. Yamanaka(2008) determined the focal depth of the off Ibaraki Pref. earthquake at 19km from the teleseismic analysis in NGY seismology note No.7. The focal depth might be shallower than 50km. However, the influence of the source process remains unsolved because we assumed the point source despite of  $M=7.0$ .

Keywords: Long-period seismic ground motion, Kanto plain, Sedimentary basin, Three-dimensional simulation, Broadband strong motion observation, Off Ibaraki Pref. earthquake in 2008

SSS023-P17

Room:Convention Hall

Time:May 24 16:15-18:45

## Long-Period Ground Motion in the Tokyo Bay area from the Chichi-jima Kinkai earthquake ( $M_j=7.4$ ) of Dec. 22, 2010.

Tomiichi Uetake<sup>1\*</sup>

<sup>1</sup>Tokyo Electric Power Company

The shallow large event of  $M_j=7.4$  occurred in Chichi-jima kinkai region on Dec. 22, 2010. The ground motion records of the event observed in the Tokyo bay area had long duration and were rich in the long-period motions. In this article, the characteristics of the records were described.

Tokyo Electric Power Company has 13 observation stations around the Tokyo bay area. 5 stations are located on the east shore and 8 stations are located on the west shore. The velocity type sensors are used in observation. The event trigger system was adopted for recording the data. Sensors had been installed on the basement of low-storied buildings and this condition did not disturb the observation of the long-period ground motions. The epicenter distance was ranged from 990 km to 1,030 km and the azimuth was ranged from 337 to 340 degree.

The duration time of the records was over 1,800 s and many later arrivals were identified. The waveform characteristics are different between the eastern side and western side. There were large later arrivals about 180 s after S wave arrival in the waveforms of eastern side and the characteristics of this wave packet were different among the observation points. On the other hand, there were no significant later arrival in the waveforms of west side. The peak velocities of the horizontal motion were 1.1-1.7cm/s in the east side and 0.5-0.8 cm/s in the west side. On the other hand, as for the up-down motion, the peak velocities were 0.2-0.3 cm/s at all stations. Peak ground velocity was recorded in the later arrival part composed of surface waves more than 180 s after the S wave arrival.

The results of multiple filter analysis showed that the later arrivals consisted of the motion in period of around 10 s. The predominant period of Ooi station in west side was about 8 s and that of Anesaki station in the east side was longer than 10 s.

The smoothed peak in period range from 8 to 12 s was shown in the velocity response spectra of 5% damping factor of the west side stations. The steep peak at period of 10 s was shown in the velocity response spectra of the east side stations. The peak value of east side stations were 6-9 cm/s and it was more than double in comparison with the peak value of west side. This difference became more remarkable in the response spectra with low damping factor. In the response spectrum with 0.1% damping factor, the peak value was around 10cm/s at the stations in west side but the value at the stations in the east side reached 30cm/s. But no significant peak was shown in the vertical component, and the response value of the vertical motion was small in comparison with the horizontal motion. It is around 2cm/s in case of 0.1% damping factor and 1cm/s in case of 5% damping factor.

In addition, the peak response time of response waveform with low-damping factor showed the large delay from the peak value time of velocity and acceleration. The duration of acceleration wave form was about 1 minutes, it was important that the peak response of the structure with low-damping factor was late for many minutes from the peak acceleration time.

Keywords: Long-period Ground Motion, Tokyo Bay Area, Chichi-jima Kinkai Earthquake, Response Spectrum

# Japan Geoscience Union Meeting 2011

(May 22-27 2011 at Makuhari, Chiba, Japan)

©2011. Japan Geoscience Union. All Rights Reserved.



SSS023-P18

Room:Convention Hall

Time:May 24 16:15-18:45

## Regional characteristics of the long-period ground motion observed at the super-dense seismic observation network

Hiromitsu Nakamura<sup>1\*</sup>, Takashi Kunugi<sup>1</sup>, Shin Aoi<sup>1</sup>, Hiroyuki Fujiwara<sup>1</sup>, Hideki Nishiyama<sup>2</sup>, Akihiko Watanabe<sup>2</sup>, Masafumi Iwata<sup>3</sup>, Atsuko Nakai<sup>3</sup>, Toshihiko Hayakawa<sup>4</sup>

<sup>1</sup>NIED, <sup>2</sup>MELTEC, <sup>3</sup>Mitsubishi Electric Corporation, <sup>4</sup>MSS

The 2003 Tokachi-oki earthquake caused great damage to oil storage tanks in Tomakomai about 250km away from the epicenter. The damage was found to be caused by sloshing excited by long-period ground motion. The 2004 Niigata-ken Chuetsu earthquake caused damage to many elevators of skyscraper buildings in Tokyo Metropolitan area some 200km away from the epicenter since the long-period ground motion resonated with these buildings. These types of earthquake damage confirmed the importance of countermeasures for long-period ground motion. The earthquake-proof elevator guideline for the skyscraper buildings recommended the elevator control systems that respond to long-period ground motion. However, these systems are not adequately installed to the existing skyscraper buildings because the costs of their installation and maintenance are expensive. On the other hand, since the long-period ground motion is less affected by the local site effects, the warning system of long-period ground motion for the skyscraper buildings will be developed inexpensively by using data observed around these buildings (around-site warning system). For the purpose of the development of the around-site warning system, we evaluate the regional characteristics of the long-period ground motion response observed at the super-dense seismic observation network (SUPREME).

Keywords: strong motion observation, long-period ground motion, K-NET, skyscraper, elevator, warning system

SSS023-P19

Room:Convention Hall

Time:May 24 16:15-18:45

## Estimation of Underground Structure with Pseudo-Inverse Matrix Calculation

Yusuke Imaeda<sup>1\*</sup>, Hitoshi Morikawa<sup>1</sup>

<sup>1</sup>Tokyo Institute of Technology

To estimate the underground structure, we usually use the observational data of gravity anomaly. We can write the relation between the density anomaly underground and the gravity anomaly at the surface as  $Ax=b$ , where vector  $x$  represents the density anomaly, vector  $b$  is the gravity anomaly, and matrix  $A$  is defined by Newton's law of universal gravitation, respectively. This relation is linear, and the reconstruction of density structure from the gravity anomaly can be expected with matrix inversion.

To perform the matrix inversion, we introduce the Moore-Penrose pseudoinverse  $A^+$ , since the number of observation data  $N$  and the number of model point  $M$  are usually different. The theory shows that matrix  $A$  can be decomposed as  $A = USV^T$ , where matrix  $U$  and  $V$  are orthogonal matrices, and  $S$  is a diagonal matrix, whose diagonal elements are singular values  $s_i$ . The Moore-Penrose pseudoinverse  $A^+$  is defined as  $A^+ = VS^+U^T$ , where  $S^+$  is the diagonal matrix, whose diagonal elements are  $1/s_i$ .

In the calculation of matrix  $V$ , the eigenvectors calculation of  $A^T A$  is needed. It is usually performed by QR algorithm, whose computational cost is of the order of  $O(M^3)$ . Since this part is the most time consuming part in the program, we adopt the I-SVD algorithm instead of traditional QR algorithm. I-SVD algorithm is a good algorithm and the computational cost is  $O(M^2)$ . Unfortunately, the next time consuming part of pre-transformation procedure is  $O(M^3)$ . So, the total computational cost remains  $O(M^3)$ .

The matrix inversion, in the terms of underground estimation, is sometimes ill-conditioned. In such case, a round-off error becomes important. Therefore, we introduce the multiple precision arithmetic or arbitrary-precision arithmetic library in our program. The round-off error can be minimised. Since we can easily switch off this option in the program, the comparison between the multiple precision calculation and the usual double precision calculation with the same program is also easy. Various tests show that the introduction of approximate pseudoinverse, whose diagonal elements less than the noise level in the observation data are replaced by 0, gives good results. The optimisation of computational speed by minimising the multiple precision calculation and the evasion of the ill-conditioned problem by introducing an new physics, such as the magnetic data, are the future work.

Keywords: density structure, gravity survey, inversion, pseudoinverse

# Japan Geoscience Union Meeting 2011

(May 22-27 2011 at Makuhari, Chiba, Japan)

©2011. Japan Geoscience Union. All Rights Reserved.



SSS023-P20

Room:Convention Hall

Time:May 24 16:15-18:45

## Prediction of average S-wave velocity for deep subsurface structure from fundamental mode Rayleigh wave phase velocity

Tatsuya Itoi<sup>1\*</sup>

<sup>1</sup>The University of Tokyo

In this paper, an empirical relationship between phase velocity for fundamental mode Rayleigh wave and average S-wave velocity of deep subsurface structure.

It is evaluated numerically using three-dimensional subsurface structure model proposed by National Research Institute for Earth Science and Disaster Prevention (Fujiwara, 2009). First, one-dimensional subsurface structure model is extracted from the three dimensional model. Then, phase velocity for fundamental mode Rayleigh wave in horizontally-layered medium is calculated for wavelength from 100 to 1000 meters using a program provided by Hisada (1997).

Calculated phase velocities are similar to average S-wave velocities in most cases. An average S-wave velocity over a certain length is empirically about 1.1 times as large as a phase velocity with the same wavelength.

It is expected that Average S-wave velocity, or S-wave profile, will be constructed with reasonable accuracy from micro-tremor array observation on ground surface in near future.

Keywords: Rayleigh wave, Average S-wave velocity, Deep subsurface structure, Phase velocity

SSS023-P21

Room:Convention Hall

Time:May 24 16:15-18:45

## Estimation of Complex Spectral Ratio of Surface and Borehole Seismometry and Numerical Tests

Kunikazu Yoshida<sup>1\*</sup>

<sup>1</sup>Geo-Research Institute

I compared 4 estimation methods of complex spectral ratios from seismic vertical array records and the results of numerical tests of noise-added synthetic records by these methods. Phase difference spectra are useful to identify velocity and attenuation structure using the spectral ratios. Examined estimation methods are two least-square approaches ( $H_1$  and  $H_2$ ), a geometrical mean of  $H_1$  and  $H_2$  ( $H_3$ ), and geometrical mean of the Fourier spectra ( $H_G$ ). These methods are different ways of assumption of noise.

The two least-square approaches assume that one of the surface or borehole records ( $y(f)$  and  $x(f)$  in the frequency domain, respectively) includes noise and the other one is noise-free. The least-square solution of the observational equation that is assumed that surface record  $y(f)$  includes noise is  $H_1=C_{xy}(f)/S_{xx}(f)$ , where  $C_{xy}$  is the ensemble mean of the cross spectra of  $x(f)$  and  $y(f)$  and  $S_{xx}$  is the one of the power spectra of  $x(f)$ . The solution that borehole records includes noise is  $H_2=S_{yy}(f)/C_{yx}(f)$ , where  $S_{yy}$  is the ensemble mean of the power spectra of  $y(f)$ . Phase difference spectra of  $H_1$  and  $H_2$  are identical.

The effects of the noise are shown in the expected value. The noise is no effects on the expected value of  $C_{xy}$ . This causes that the phase differences are expected to be robust. The expected values of  $S_{xx}$  and  $S_{yy}$  are affected by the variance of the noise of  $x(f)$  and  $y(f)$ , respectively. This indicates that the  $H_1$  and  $H_2$  are different for the same  $x(f)$  and  $y(f)$ .

I applied these 4 methods to estimate the spectral ratios of the spectra of noise-added synthetic surface and borehole records. The noise-free surface and borehole synthetic records were calculated with the exact transfer function of the vertically incident plain wave in the homogeneous medium with the surface. I made noise-added synthetic records by adding 20 different white noise on the noise-free synthetic records.

Stacked spectral ratios were calculated by the 4 methods. Mean values of cross and power spectra of the 20 pairs of noise-added synthetics were calculated.  $H_1$ ,  $H_2$ , and  $H_3$  were calculated from the mean values.  $H_G$  were calculated with geometrical mean of the spectral ratios of the Fourier spectra  $y(f)/x(f)$ . The result of  $H_1$  indicates small error in the frequencies between peaks of the exact transfer function, whereas, at the peak frequency of the transfer function,  $H_1$  underestimates the peaks due to the noise in the borehole records.  $H_2$  indicates clear peaks, whereas it overestimate the valleys.  $H_3$  are the geometrical mean value that is robust, but indicates unclear peak compared with  $H_2$ .  $H_G$  are close to  $H_3$ . Phase difference spectra of  $H_1$  and  $H_2$  are very close to the exact transfer function.

Smoothed spectra of noise-free synthetic spectra are very similar to the stacked spectra.  $H_1$ ,  $H_2$  and  $H_3$  were calculated from smoothed cross and power spectra.  $H_G$  are the geometrical mean of the spectral ratios of the smoothed Fourier spectra  $x(f)$  and  $y(f)$ . Parzen window was used as a smoothing window. The spectra applied both of stacking and smoothing also results similar to the stacked spectra.

Keywords: seismic vertical array, complex spectral ratio, transfer function



SSS023-P22

Room:Convention Hall

Time:May 24 16:15-18:45

## Estimating small-scale site effect as functions of the frequency range from 2 to 4Hz by observing microtremors

Torao Tanaka<sup>1\*</sup>, Makoto OKUBO<sup>1</sup>, harumi aoki<sup>1</sup>

<sup>1</sup>TRIES

Remarkable amplifications of seismic waves caused by shallow ground soil generate seismic damages. The frequency of characteristic vibrations of popular wooden houses in Japan ranges from 2 to 4Hz and is same to the range of the seismic magnification of shallow ground soil, and may be called the site effect. Accordingly it is essential for mitigation of seismic hazards to estimate the site effect quantitatively in detail within the area concerned. Since the observation of microtremor amplitudes is comparatively simple and carried out anytime, it will be one of effective and simple methods, if the observed amplitudes are significantly related with those of the maximal amplitudes of seismic waves. Thus we have investigated the spectral characteristics of acceleration records observed at TRIES network. Analyzed data are the amplitudes of microtremors, the biggest part of surface waves caused by distant and large earthquakes such as the 2004 Off Kii Peninsula Earthquakes and S waves by local and small earthquakes observed at the same network since 1999. We calculated spectral amplitudes of microtremors, the surface and S waves by Fourier transform. Spectral amplitudes of microtremors were obtained from the same seismograms recorded during about 10 seconds from the start of recording by the trigger signal to the arrival of initial seismic P wave. We define the site effect as a magnification function of seismic spectral amplitudes in the three directions of UD, NS or EW, depending on the frequencies in the range of 2 to 4Hz. Since our investigations depend on the stationarity of the spectral amplitudes of microtremors at the point concerned, it is fundamental to show that our assumption holds with high credibility, as well as mitigation of seismic hazard by using our site effect will be possible or not. Though preliminary analyses of microtremor amplitudes give a credibility of about 70% of the seismic magnification, we are continuing further data analyses of the relation between maximal seismic waves and microtremor amplitudes.

Keywords: microtremor, ground soil, site effect, characteristic oscillation, Fourier transform, maximal amplitude

SSS023-P23

Room:Convention Hall

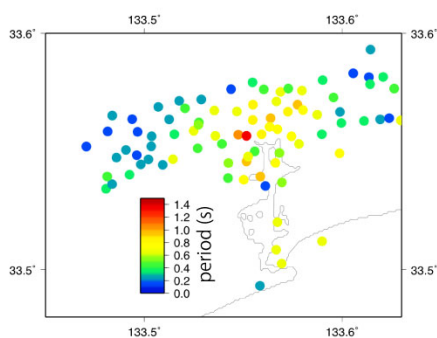
Time:May 24 16:15-18:45

## Spatial distribution of predominant period derived from H/V spectra in Kochi Plain

Atsuki Kubo<sup>1\*</sup>, Sawa Tajima<sup>2</sup>, Tadashi Hara<sup>3</sup>

<sup>1</sup>Earthq. Obs. Fac. Sci. Kochi Univ., <sup>2</sup>Fac. of Sci. Kochi Univ., <sup>3</sup>Sect. of Disast. Prev. Kochi Univ.

If the Nankai Earthquake occur, Kochi city will be damaged by both strong ground motion and submergence due to ground subsidence and Tsunami. These disasters will be concentrated in thick sediment region and/or high subsidence region. Thus sediment/Basement structure around the Kochi city is important to understand nature of the disasters. We conducted microtremor observation around Kochi city. We used JU210 seismometer for microtremor by Hakusan Coop. We observed microtremor 88 points around Kochi city and analyzed H/V spectra. Obtained dominant period distribution is shown in Figure. Both ends of east-west extending Kochi plain, short period dominant frequencies are recognized (western region 0.3s or less; eastern Kochi city 0.6s or less). In contrast, central region faced to Urato-Bay area, longer period distribution are observed (larger than 0.6s up to 1.45s). Structure modeling to explain these observations is important issue in future study. In central area faced to Urato-Bay, provision for both submergence and strong ground motion with longer dominant period.



Keywords: Micro tremor, Predominant Period, Surface Basement, Kochi Plain

SSS023-P24

Room:Convention Hall

Time:May 24 16:15-18:45

## Estimation of subsurface structure using microtremor H/V spectral ratio in the Shimabara peninsula

Natsumi Itoya<sup>1\*</sup>, Takeshi Matsushima<sup>1</sup>

<sup>1</sup>SEVO, Kyushu University

Recently, the estimation of long-period strong ground motions is getting more important in accordance with construction of large-scale building structures. According to the contour map of peak period in the long-period ground motions in Japan (the Central Disaster Prevention Council, 2008), they estimated that the long-period ground motions are amplified not only in sedimentary basin like the Kanto plains in the central Japan, but also in volcanic area of the Shimabara peninsula in Kyushu, Japan. Especially, in the Yadake region of the center part of the peninsula, the long-period ground motions amplify to the same extent as Tokyo area in the Kanto plains. In order to estimate a ground structure in the Shimabara peninsula by paying attention to microtremor H/V spectra (horizontal-to-vertical spectral ratio) as an evaluation method of the ground structure, we carried out microtremor observations at 60 points in the whole area of Shimabara peninsula.

The microtremor observations using a three-components wideband portable seismometer of characteristic period 120 second were carried out at each observation site. The data of microtremor were recorded by a portable data-logger with 100Hz sampling.

Power spectrum of UD, NS, and EW were calculated and smoothed by using the ensemble average of thirty times, and power ratio of the horizontal and vertical spectrum (H/V spectra) was estimated, where the horizontal spectra are the geometric mean of the NS and EW components.

By using data from 60 observation sites, we traced a contour map of primary natural peak period (the longest peak period that exists from 1 to 10 seconds). Peak period of 5-6 s in H/V spectra was obtained at a lot of observation sites at east side of the Shimabara peninsula, where volcanic sediments are thickly distributed. It is thought that the thick volcanic sediment layer is a cause of such longer peak period in H/V spectra.

In the central western area of the Shimabara Peninsula, there are no remarkable peaks in the observed H/V spectra. According to explosion seismic research (Explosion seismic research group of Unzen Volcano, 1995), this area corresponds to rock layer having  $V_p=3.5\text{km/s}$ , which distributed in shallow to ground surface as a solid lava layer. This structure is reflected in shape of H/V spectra; the value of H/V spectra in this area is nearly constant in the frequency of microtremor.

Next, we are going to estimate subsurface structures in the peninsula using the observed H/V spectra. Using P wave velocity that had been obtained by the explosion seismic research, S wave velocity and density were calculated by relation estimated by Ludwig et al. (1970). During a trial-and-error estimation process, S wave velocity, P wave velocity and density were fixed, and we adjusted the thickness of the sedimentary layers to find a reasonable fit of primary natural peak period of the calculated H/V spectra and the observed H/V spectra to determine the ground structure. Then, the depth to  $V_s=600\text{m/s}$  layer is estimated as 1.2km at the boring site USDP2 in east side of Shimabara peninsula. Our result is consisting with boring-core sampling data from the borehole.

The horizontal component of long-period microtremor, locally exceed in Yadake site of the center part of Shimabara peninsula. If the ground structure is determined by using the same parameter as surrounding sites, the depth to the basement in Yadake site should be estimated as about 1000 m. However, nearby tectonic map and the result of explosion seismic research do not show such a steep basin structure under Yadake site. Thus, we changed S wave velocity of shallow part of the underground structure, and we found that the very low-velocity layer exists beneath surrounding of Yadake site. Because the rich hot-spring sources exist in around the Yadake site, it is thought enough that existence of the low-velocity layer, which causes the increase of the long-period strong ground motions.

Keywords: microtremor, H/V spectral ratio, subsurface structure, long-period ground motion

SSS023-P25

Room:Convention Hall

Time:May 24 16:15-18:45

## Period-Dependent Site Amplification and Source Process for the 2008 Iwate-Miyagi Nairiku, Japan, Earthquake Sequence

Rami Ibrahim<sup>1\*</sup>, Kazuki Koketsu<sup>1</sup>, Hiroe Miyake<sup>1</sup>, Kazuhito Hikima<sup>2</sup>

<sup>1</sup>Earthq. Res. Inst., Univ. Tokyo, <sup>2</sup>TEPCO

The 2008 Iwate-Miyagi Nairiku earthquake on 14 June 2008 mainly struck the Tohoku region, northeastern Japan. The JMA magnitude  $M_{JMA}$  was estimated to be 7.2 and the moment magnitude  $M_W$  by Global CMT Project was 6.9. The 5% damped acceleration and velocity response spectra maps reveal different features in the source area and at other stations out of the source area. The predominant period was shown in a short period range of 0.1-0.2 s. AKTH04 station which is located at 22 km away from the source area was recorded a JMA-intensity of 6 upper as large as in the source area. The large acceleration amplitude was observed at short periods at the same station. Large velocity amplitudes at stations MYG005 and MYG006 were observed at periods of 2, 3, and 5 s to the south of the source area. In this study, we use aftershock data to obtain amplification factors in and around the source area. The H/V spectral ratios were investigated at 27 station sites close to the source area. The data recorded by K-NET and KiK-net were used for five aftershocks. The spectral ratios of the horizontal components (H/H spectral ratio) of surface and borehole data were investigated for KiK-net stations. H/H spectral ratios of soft soil sites to hard rock sites were also calculated for comparison with previous studies. Amplification factors of 3 to 6 at short periods of 0.1 to 0.5 s are observed at many stations such as AKTH04, AKTH06, IWTH19, and so on. The stations of MYG005, MYG006, IWT011 and IWTH20 have shown amplification factors of 3 to 5 at long periods of 3 to 5 s. On the other hand AKT023, IWT010, and MYGH04 show flat response spectra compared to hard rock sites. The results reveal that the different features shown by response spectra can be attributed to the site effects. The H/V and H/H spectral ratios were used to get information about the predominant periods and the amplification factors at the station sites. The peak velocity amplitude distribution maps were calculated for different period ranges of 0.1-0.2, 0.2-0.3, 0.3-0.5, 0.5-1, 1-2, 2-3, 3-5, and 5-10 s. We are going to collect site amplification factors for the mentioned period ranges. The collected data will be used to retrieve the period-dependent source process for the 2008 Iwate-Miyagi Nairiku earthquake.

Keywords: 2008 Iwate-Miyagi Nairiku earthquake, source process, amplification

# Japan Geoscience Union Meeting 2011

(May 22-27 2011 at Makuhari, Chiba, Japan)

©2011. Japan Geoscience Union. All Rights Reserved.



SSS023-P26

Room:Convention Hall

Time:May 24 16:15-18:45

## Microtremor array survey in southern Osaka plain

Masayuki Yoshimi<sup>1\*</sup>, haruko Sekiguchi<sup>2</sup>, kimiyuki Asano<sup>2</sup>, haruo Horikawa<sup>1</sup>, tomotaka Iwata<sup>2</sup>, haruo Kimura<sup>1</sup>

<sup>1</sup>Geological Survey of Japan, AIST, <sup>2</sup>DPRI, Kyoto Univ.

We conducted microtremor array survey at six locations in southern Osaka plain using 7 to 10 velocity seismometers arranged to multi-triangle array. Applying SPAC and E-SPAC method to the observed data, we estimate phase velocities (dispersion curves) from 0.3-0.5 km/s up to 1.0-1.5 km/s at frequency range 3-5 Hz down to 0.3-0.5 Hz. Then, S-wave velocity structures satisfying the dispersion curves are searched using GA method, assuming three layers ( $V_s=0.35, 0.55, 1.0$  km/s) or gradually increasing velocity structure overlaying seismic bedrock ( $v_s=3.2$ km/s). As a result, we successfully obtain velocity structures of which depths to the bedrock consistent with previous studies.

### Acknowledgement

This research is funded by Integrated research project for the Uemachi active fault system by MEXT.

Keywords: SPAC method, S wave velocity structure, GA

# Japan Geoscience Union Meeting 2011

(May 22-27 2011 at Makuhari, Chiba, Japan)

©2011. Japan Geoscience Union. All Rights Reserved.



SSS023-P27

Room:Convention Hall

Time:May 24 16:15-18:45

## Explorations of S-wave velocity structure around the K-NET stations in Ishigaki and Iriomote island, Japan

Nobuyuki Yamada<sup>1\*</sup>, Hiroshi Takenaka<sup>2</sup>, Ryota Okudaira<sup>2</sup>, Fuminori Goto<sup>2</sup>, Toshihiro Kuramoto<sup>2</sup>

<sup>1</sup>Fukuoka University of Education, <sup>2</sup>Kyushu University

We conducted microtremor array measurements for the 3 sites in the Ishigaki island and Iriomote island to estimate 1D S-wave velocity profiles of deep sedimentary layers over the basement with a  $V_s$  about 3.0km/s. In this presentation, we will discuss the details of the observation and analysis. We will analyze the data and get the S-wave velocity profiles at the 3 sites.

Keywords: Microtremor array measurements, S-wave velocity structure, Ishigaki & Iriomote Islands

# Japan Geoscience Union Meeting 2011

(May 22-27 2011 at Makuhari, Chiba, Japan)

©2011. Japan Geoscience Union. All Rights Reserved.



SSS023-P28

Room:Convention Hall

Time:May 24 16:15-18:45

## Determination of subsurface structure of Tottori dunes and around Koyama Pond in Tottori Plain from Microtremor Observat

Yusuke Ishida<sup>1\*</sup>, Yuhi Onaga<sup>1</sup>, Tatsuya Noguchi<sup>1</sup>, Takao Kagawa<sup>1</sup>

<sup>1</sup>Tottori University

Microtremor observations were conducted in the area of the north / the east bank level of Koyama Pond and Tottori dunes in Tottori Plain. The area has been developed since late 20th century. Three components observations were carried out for surveying predominant period distribution in the area. H/V spectral ratios are used to obtain predominant period at observation sites. Array observations were also executed in the area. Alternatively, SPAC method and CCA method are applied for 4 or 5 stations arrays with diameter 2.5 to 50 meters. Through the study, obtained predominant period distribution agrees well with past topographies. Subsurface structures derived from array observation consist with borehole data, previous explorations, and the predominant periods coincide with analysis result mentioned above. Following the results, we are interested in the underground structure beneath Koyama Pond. It is important to reveal the structure to conduct simulations of wave propagation in this area.

Keywords: Microtremor, Tottori dunes, Koyama Pond, subsurface structure

# Japan Geoscience Union Meeting 2011

(May 22-27 2011 at Makuhari, Chiba, Japan)

©2011. Japan Geoscience Union. All Rights Reserved.



SSS023-P29

Room:Convention Hall

Time:May 24 16:15-18:45

## Determination of underground structure of Padang, Indonesia by microtremor observations

Tatsuya Noguchi<sup>1\*</sup>, Shuji Uemura<sup>1</sup>, Atsushi Sato<sup>2</sup>, Rusnardi Rahmat Putra<sup>2</sup>, Yusuke Ono<sup>1</sup>, Junji Kiyono<sup>2</sup>, Tatsunori Ikeda<sup>2</sup>, Takao Kagawa<sup>1</sup>

<sup>1</sup>Tottori Univ., <sup>2</sup>Kyoto Univ.

Serious damages occurred by the strong ground motions during the 2009 Southern Sumatra earthquake in the area. Microtremor observations have been carried out in Padang, Indonesia and determined a subsurface structure by Noguchi et al. (2010). The deep S-wave velocity structure models at the 3 sites were determined from array observation records. The predominant period at 63 sites were obtained from 3-component observation records. S-wave velocity of a bottom bedrock layer is 1500m/s and depth to the bedrock was about 200m maximum from obtained underground model at 3 sites array observation. The predominant period was 1.5-3.0 period that H/V spectral ratio has clear single peak and double peaks. It was found that soft alluvial layer was distributed whole area from S-wave velocity structure.

Keywords: Microtremor observation, S-wave velocity structure, H/V, Padang, Indonesia



SSS023-P30

Room:Convention Hall

Time:May 24 16:15-18:45

## Estimation of velocity structure using seismic interferometry at Hsinchu, Taiwan

keitaro matsumoto<sup>1\*</sup>, Hitoshi Morikawa<sup>1</sup>, Masachika Tanigawa<sup>1</sup>, Huei-Tsyr Chen<sup>2</sup>, Tsao Jung-Kai<sup>2</sup>

<sup>1</sup>Tokyo Institute of Technology, <sup>2</sup>National Central University

Hsinchu is one of important areas in Taiwan, because there are many IT and IC industries are located and they are most important resources for Taiwanese economy. We can remember that the price of memories for computers has jumped up immediately after the 1999 Chi-Chi earthquake. This means that the business continuity plan (BCP) for the companies in this area is critical issue for the Taiwanese economy. For this purpose, we need an appropriate estimation of earthquake ground motion in a specific site, however, enough information is not available until now.

We have continued to model a ground structure around this area to apply to an estimation of earthquake ground motion. Shosaka et al. (2007) proposed three-dimensional shape of bedrock based on the gravity survey. In their model, the depth to the bedrock is deeper in the south-eastern mountainous area than in the north-western seashore area. To confirm this results, Kawatsure et al. (2009) and Iwahori et al. (2009) carried out array observation of microtremors, however, they could not reach the deepest bedrock because of the limitation of sensors.

Thus, to break this wall, we apply new observation systems and technique of seismic interferometry. We developed a new data logger with extremely low noise and applied simple moving-coil-type velocity sensors with 0.5-second natural period. We set 5 velocity sensors around the area with deep bedrock and observed continuously the microtremors for 50 days.

The technique of seismic interferometry was applied to the observed data, and Green's functions for vertical components are obtained among the sensors. Furthermore, applying multiple filter analysis for 7 sec to 1 sec, and the group velocities are estimated between 7 to 1 sec. In this time, although we can estimate an averaged structure between the sites, they suggested that a part of velocity structures estimated from microtremors does not agree with the density structure obtained from the gravity survey. For future analyses, we will try to explain the differences between the velocity and density structures around this area.

Keywords: Seismic interferometry, Green's function, microtremor

# Japan Geoscience Union Meeting 2011

(May 22-27 2011 at Makuhari, Chiba, Japan)

©2011. Japan Geoscience Union. All Rights Reserved.



SSS023-P31

Room:Convention Hall

Time:May 24 16:15-18:45

## Estimation of inter-station Green's functions by CEORKA continuous data for validating velocity model of Osaka basin

Takashi Akazawa<sup>1\*</sup>, Kazuhiro Somei<sup>1</sup>, Kimiyuki Asano<sup>2</sup>, Tomotaka Iwata<sup>2</sup>

<sup>1</sup>G.R.I., <sup>2</sup>DPRI, Kyoto Univ.

The Committee of Earthquake Observation and Research in the Kansai Area (CEORKA), which is arraying stations throughout the Kansai district, has obtained records from large earthquakes to small local earthquakes with taking advantage of broadband velocity seismograph. Since the observation started in April 1994, the CEORKA network has used trigger method for obtaining ground motion records. Since 2009, the committee is engaging to build new observation system, which can send continuous data in real-time, with introducing a new data logger for aiming to transmit seismic early warning in real-time.

To evaluate the accuracy of records obtained by the new data logger, the microtremor records obtained simultaneously by the data logger and SMAR-6A3P, which is widely used to microtremor observation, were compared. The results clarified that the data logger can obtain microtremor records in the frequency range of 0.2 to 30Hz. In this study, we start estimate inter-station Green's functions applying the seismic interferometry method using the continuous record obtained by the new data logger. The inter-station Green's function can be used for verification of the basin velocity model of the Osaka basin.

# Japan Geoscience Union Meeting 2011

(May 22-27 2011 at Makuhari, Chiba, Japan)

©2011. Japan Geoscience Union. All Rights Reserved.



SSS023-P32

Room:Convention Hall

Time:May 24 16:15-18:45

## Simulation for retrieving Green's function with seismic interferometry

wakana tsutsumi<sup>1\*</sup>, Hiroaki Yamanaka<sup>1</sup>, Kosuke Chimoto<sup>1</sup>

<sup>1</sup>Tokyo institute of technology

Seismic interferometry is widely used in various kinds of seismology to retrieve the Green's function from long-term ambient noise data. It is sometimes difficult to estimate proper the Green's function from actual data, such as non symmetrical correlation in negative and positive delay times. In this study we conducted numerical simulations for retrieving the Green's function from synthetic microtremor data calculated using a 3DFD code.

A surface vertical loading was set on the surface around two stations (10km apart) to simulate microtremor data. The synthetic velocities were used to generate a correlation. The correlations from 120 sources were stacked with the seismic interferometric way. We confirmed that the correlation agrees with the surface wave portions of the Green's function between the two sites. However, body wave part could not be reconstructed with the correlation. This is due to the lack of sources in vertical direction in the simulation. Since most of possible sources of microtremors are located on the surface, these phenomena can be essential in a correlation from microtremors.

We also conducted similar simulations with S-wave velocity models having irregular interfaces. We have difficulties to retrieve Green's function correctly when the basin has strong lateral heterogeneities. The vertical interface of the basin generates waves as secondary sources that violate the assumption of equal source distribution.

Keywords: seismic interferometry

SSS023-P33

Room:Convention Hall

Time:May 24 16:15-18:45

## Estimation of application conditions for seismic interferometry based on numerical simulation

Kazuhiro Somei<sup>1\*</sup>, Ken Miyakoshi<sup>1</sup>, koji hada<sup>2</sup>

<sup>1</sup>G.R.I, <sup>2</sup>NewJec Inc

The seismic interferometry reconstructs the pseudo shot record (Response function) from observed seismic data simultaneously by auto-correlation or cross-correlation function. The Response function provides us with useful information for imaging the subsurface structure. However, it is important to evaluate the applicability of this technique. One of the conditions of response functions is characterized by filtering or source characteristics of the observed seismic data. In this study, we examined the application conditions for the seismic interferometry estimated from auto-correlation by using theoretical waves. Next we also applied it to the observed strong motion records in the Osaka basin.

First, we examined the appropriate frequency range of the response function corresponded with the depth of the basement structure. Assuming the basement structure model beneath a receiver, we calculated theoretical waveforms with a variety of rise times and filtering. The Green's function is calculated by using discrete wavenumber method (Bouchon, 1981) with the reflection and transmission matrix (Kennett and Kerry, 1979). We obtained a sufficient database for various frequency range and rise time for imaging an assuming depth of the basement. The appropriate rise time is less than 0.5s to estimate basement depth from 100 m to 1000 m. we also found that low-cut filtered waveforms by 1.0 Hz are relatively available to estimate basement depth shallower than 500 m.

Second, we compared the SN ratio of the response function with number of stacked records using above database. Signals of the response function have sufficient SN ratio with stacked records up to 50. Using the observed seismic data, however, more stacked records will be required for sufficient SN ratio because of various noises exist in the seismograms.

Finally, we applied the seismic interferometry to estimate seismic basement structure in the Osaka basin using observed strong motion records. The basement depth estimated from the seismic interferometry agrees with the basin model in the Osaka area (e.g. Kagawa *et al.*, 2004). At some station, however, especially near the edges of the Osaka basin, the depth estimated from the response functions did not agree with the Osaka basin model.

### Acknowledgements

We would like to sincerely thank NIED (K-NET, KiK-net) for providing the strong motion data. The hypocenter information was providing by JMA and moment tensor by F-net of NIED.

Keywords: seismic interferometry, auto-correlation function, numerical simulation, application conditions, Osaka basin